TR – 203

TECHNICAL REPORT

OCEANOGRAPHY IN THE CHANNEL ISLANDS AREA OFF SOUTHERN CALIFORNIA SEPTEMBER AND OCTOBER 1965

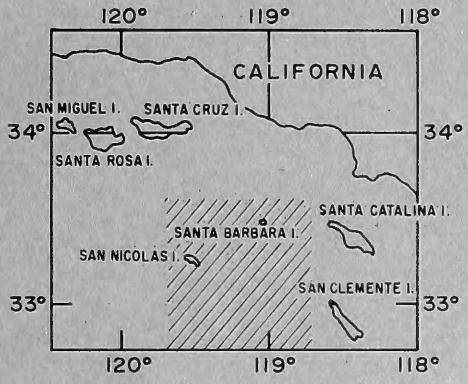

JUNE 1968

NAVAL OCEANOGRAPHIC OFFICE
WASHINGTON, D.C. 20390
PRICE 90 CENTS

ABSTRACT

The Naval Oceanographic Office conducted an oceanographic survey in the Channel Islands area aboard USNS DAVIS (T-AGOR 5) during September and October 1965. The survey was a detailed environmental study with major emphasis on currents, sound velocity structure, and bottom composition. Physical, chemical, geological, and biological data were collected.

Seaward decreases in surface temperature and salinity depicted the influence of the cold, low salinity California Current on the survey area. The sound channel was bottom bounded due to the shallow depths, and the sound velocity axis occurred at a depth of 850 meters (2800 feet). Surface duct development was weak and usually restricted to the upper 10 meters (30 feet).

Data from repeated Nansen casts at anchor stations revealed temperature, salinity, and sound velocity to oscillate in a sinusoidal manner throughout a day. This oscillation is attributed to a combination of internal waves, tidal forces, and the earth's rotational forces.

Current data from parachute current drogues, current meters, and computed dynamics showed the San Nicolas Basin to be the center of a counterclockwise gyre. Maximum current speeds of about 25 cm/sec occurred around the basin periphery. Lesser speeds existed towards the center of the basin and with increasing depth. Current meters, planted 2 miles northeast of San Nicolas Island, indicated a clockwise rotational water movement produced by the tides.

Both bottom sediment analyses and bottom photographs showed the survey area to have the same general characteristics as have been observed in previous studies. Fine-grained, green-gray muds

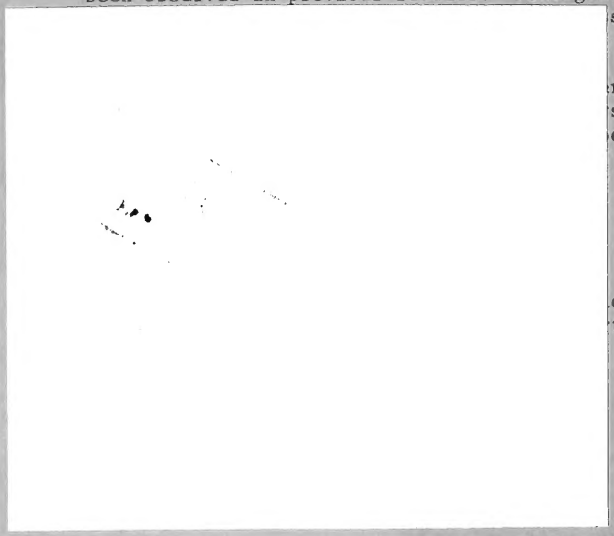

sions, and somewhat

r and several in October,
s suggested that the
er and the second week

on
tment

FOREWORD

The Naval Oceanographic Office conducted a detailed environmental study in the Channel Islands area during September and October 1965. Major emphasis was placed on currents, sound velocity structure, and bottom composition. The proximity of the ocean stations to each other on this survey allows a synoptic description of the data obtained. This technical report describes the effects on the ocean environment produced by the California Current, daily tides, earth's rotation, and internal waves. Also presented are discussions of bottom composition and plankton distributions.

L. E. DeCAMP
Captain, U.S. Navy
Commander

CONTENTS

		Page
I.	INTRODUCTION	1
II.	NARRATIVE OF OPERATIONS	2
III.	METHOD OF PROCEDURES	4
	A. Instrumentation and Data Collection	4
	1. Nansen Cast	4
	2. Sound Velocimeter	4
	3. Parachute Current Drogue	4
	4. Current Meter	5
	5. Bottom Sediment	5
	6. Bottom Photography	6
	7. Plankton	6
	8. Bathythermograph	6
	B. Data Processing and Presentation	6
IV.	PERSONNEL AND ACKNOWLEDGMENTS	7
V.	DATA ANALYSIS	7
	A. Temperature	7
	B. Salinity	9
	C. Dissolved Oxygen	11
	D. Sound Velocity	12
	1. Computed Sound Velocity from Nansen Cast Data	12
	2. Comparison of Nansen Cast and Ramsay Velocimeter Methods	13
	3. Discussion of Other Sound Velocity Influences	14
	E. Currents	16
	1. General	16
	2. Parachute Current Drogues	16
	3. Current Meters	23
	4. Dynamic Topography	28
	5. Summary of Water Circulation in the Channel Islands Area	29
	F. Bottom Composition	30
	1. Core Analysis	30
	2. Bottom Photography	31
	G. Biological Analysis	35
VI.	SUMMARY AND CONCLUSIONS	46
VII.	BIBLIOGRAPHY	49

FIGURES

		Page
1.	Topographic Features of the Survey Area	1
2.	Station Locations of Oceanographic Operations	3
3.	Parachute Current Drogue Assembly	5
4.	Current Meter and Array	5
5.	Representative Temperature Versus Depth Profiles	7
6.	Horizontal Temperature Distributions	8
7.	Representative Salinity Versus Depth Profiles	9
8.	Horizontal Salinity Distributions	10
9.	Representative Oxygen Versus Depth Profile	11
10.	Horizontal Oxygen Distributions	12
11.	Representative Sound Velocity Profile from Nansen Cast Data	12
12.	Nansen Cast Sound Velocity Versus Time at 400 Meters	13
13.	Ramsay Probe Sound Velocity Versus Time at 400 Meters	14
14.	Comparison of Nansen Cast and Ramsay Probe Sound Velocities	14
15.	Relation of Sound Velocity with High and Low Tides - Anchor Station 1, October	14
16.	Relation of Sound Velocity with High and Low Tides - Anchor Station 2, October	15
17.	Parachute Drogue Tracks - Launch Site 1	17
18.	Parachute Drogue Tracks - Launch Site 2	18
19.	Parachute Drogue Tracks - Launch Site 3	19
20.	Parachute Drogue Tracks - Launch Site 4	20
21.	Parachute Drogue Tracks - Launch Site 5	21
22.	Counts Versus Rotor Speed for Current Meters at 30 and 50 Meters	25
23.	Polar Coordinate Plots for Current Meters at 30 and 50 Meters	25

FIGURES (Cont'd)

Page

24. Rotor Speed Versus Direction for Current Meters at 30 and 50 Meters....25

25. Current Meter Velocity Components at 30 Meters with Computed Tides for the Four Phases of the Moon....26

26. Current Meter Velocity Components at 55 Meters with Computed Tides for the Four Phases of the Moon....27

27. Topography of the 0-, 50-, and 100-Decibar Surfaces Relative to the 500-Decibar Surface....28

28. Circulation Patterns From Drogues, Current Meters, and Dynamics - September and October 1965....29

29. Sequential Series of Bottom Photographs From Camera Lowering Number 1....32 through 34

30. Representative Bottom Photographs From Camera Lowering Number 2....36

31. Representative Bottom Photographs From Camera Lowering Number 3....37

32. Representative Bottom Photographs From Camera Lowering Number 4....38

33. Plankton Distribution....41 through 45

TABLES

I. Drogue Velocity Summary....22

I. INTRODUCTION

The Naval Oceanographic Office (NAVOCEANO) conducted an oceanographic survey in the Channel Islands area aboard USNS DAVIS (T-AGOR 5) during September and October 1965. The survey area encompassed the San Nicolas Basin, San Nicolas Island, and Santa Barbara Island (Fig. 1).

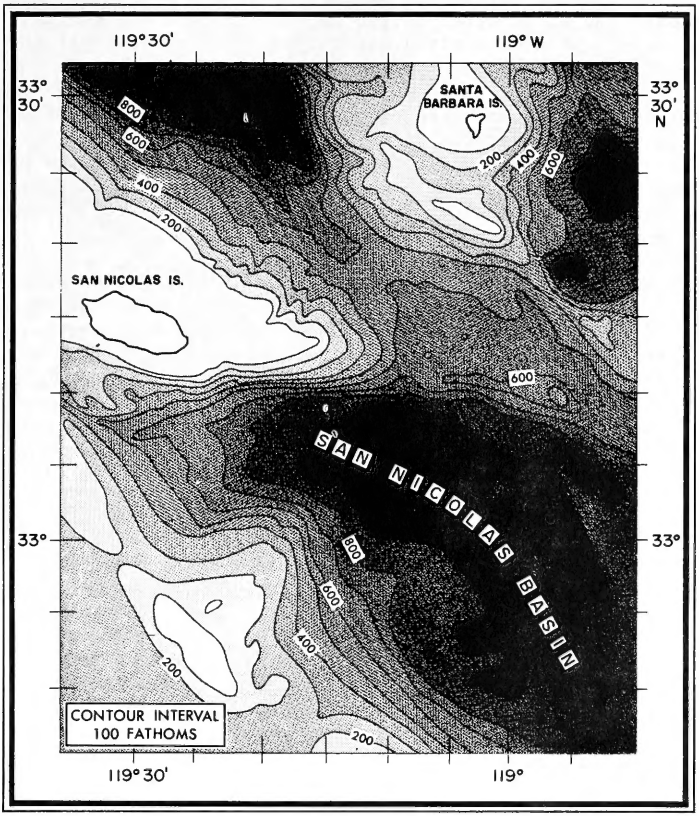

FIGURE 1. TOPOGRAPHICAL FEATURES OF THE SURVEY AREA

The survey was a detailed environmental study with major emphasis on currents, sound velocity structure, and bottom composition. In addition, fluctuations of various oceanographic parameters were studied in relation to the effects of the phases of the moon on the daily tides.

The submerged shelves of continents typically are gentle in slope, but the continental shelf off southern California is one of the few

areas in the world that has numerous depressions and rises. The topography is characterized by many basins, banks, and islands and has a regional physiographic trend similar to that of the adjoining land area. Some depressions reach bathyal depths and some elevations rise above water to form islands.

The south-flowing California Current dominates the surface water circulation. The great gyral motion of this current and the entrainment of deeper waters produce a mixed water type of a transitional nature (Gorsline, 1966).

Scientists have often surveyed the waters off the coast of southern California; nevertheless, the surveys have been too broad to delineate small scale oceanographic variations in this extremely complex area. At the same time, owing to the amount of oceanographic work done, there is more general knowledge of these waters than of other ocean areas of comparable size and complexity (Emery, 1960).

NAVOCEANO, at the request of the Pacific Missile Range, Point Mugu, California, conducted two earlier surveys north of the Channel Islands, off Point Arguello, California, in January and November-December 1964 (Thomas, 1968). Oceanographers occupied a grid of stations with distances between stations varying from 15 to 30 miles. The distance between stations and the 9-month interval between surveys make it impossible to determine the oceanographic variations that result from tidal activities; but, the separate studies give a good description of water circulation to a distance of 100 miles off Point Arguello.

II. NARRATIVE OF OPERATIONS

Oceanographic observations in the Channel Islands area began on 16 September and ended on 15 October 1965. Figure 2 shows the locations of all data collected on the survey.

Twenty-five Nansen stations were occupied from 21 to 24 September and reoccupied from 11 to 14 October. The station grid formed a 40-mile square with stations 10 nautical miles apart. Data from these stations included Nansen cast temperature and salinity measurements on all stations and dissolved oxygen determinations on the September stations.

Repeated Nansen casts were taken at two anchor stations. Anchor station 1 was occupied from 27 to 28 September and 9 to 10 October; anchor station 2 was occupied from 28 to 29 September and 7 to 8 October. The reversal of the October anchor stations occurred because the survey ship was nearer station 2 when the anchor stations were reoccupied.

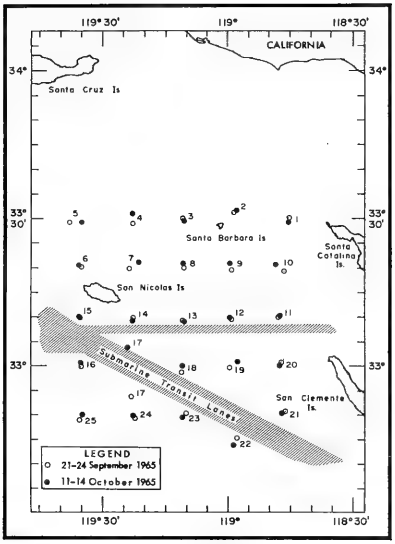

NANSEN STATIONS

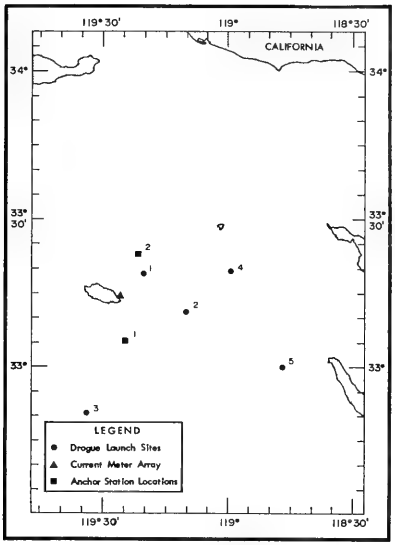

DROGUE, CURREN METER, AND ANCHOR STATIONS

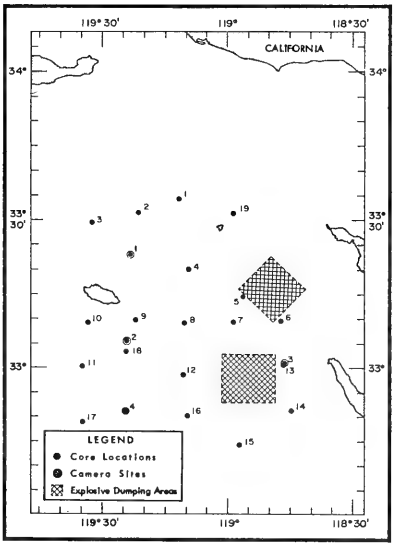

CORE AND CAMERA LOWERINGS

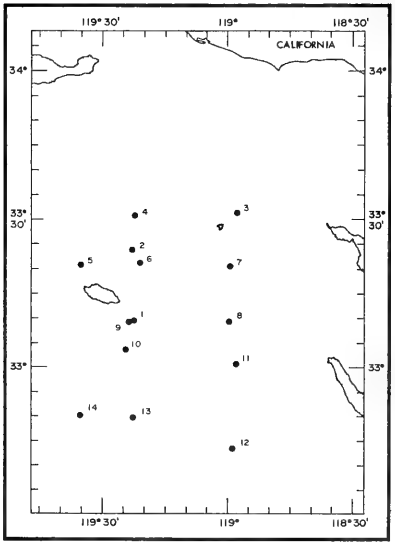

PLANKTON

FIGURE 2. STATION LOCATIONS OF OCEANOGRAPHIC OPERATIONS

Parachute current drogues were launched in sets from sites 1 to 5 on 16 and 17 September, 17 to 19 September, 25 and 26 September, 29 September to 1 October, and 10 and 11 October, respectively.

A current meter array was anchored near San Nicholas Island on 17 September and was retrieved on 15 October.

Additional data included 51 sound velocimeter lowerings, 19 bottom sediment samples, photographs from four bottom camera lowerings, 14 plankton samples, and 24 bathythermograms on Nansen stations 2 through 25 during October.

III. METHODS AND PROCEDURES

A. Instrumentation and Data Collection.

1. Nansen Cast. Serial-depth temperatures and salinities were sampled throughout the water column on standard Nansen cast stations. Attempts were made to collect data as close to the bottom as possible. Protected deep sea reversing thermometers were used on each Nansen bottle to obtain *in situ* water temperatures, and unprotected reversing thermometers were spaced throughout the casts to obtain reversal depths of the Nansen bottles.

A water sample was drawn from each Nansen bottle and analyzed for salinity aboard ship with an Industrial Instruments inductive salinometer. Salinities are considered accurate to ± 0.01 ‰.

During September, additional water samples drawn from the Nansen bottles were analyzed for dissolved oxygen content aboard ship using the NAVOCEANO modification of the Winkler method.

2. Sound Velocimeter. A Ramsay sound velocimeter, with an AGODDS printout system, was used only at anchor stations to supplement hand computed sound velocity data. The velocimeter was lowered every two hours and simultaneously with the Nansen casts which were taken every 4 to 6 hours. In the latter case, the 100-pound lead weight, normally used at the end of the oceanographic wire, was replaced by the velocimeter.

3. Parachute Current Drogue. At site 1 (Fig. 2), three drogues were launched with parachutes at depths of 5, 25, and 50 meters. At sites 2 through 5, four drogues were launched at each site with an additional drogue at 100 meters.

The drogue assembly, illustrated in Figure 3, included a 30-foot diameter parachute, a styrofoam log as the surface float, and two 10-foot aluminum poles connected together with approximately 15 feet extending above the water surface. Attached to the upper portion of the pole was a flag for day and a flashing light for night identification and a radar reflector for tracking the drogue in calm seas. A 3/32-inch

stainless steel wire rope was used to attach the parachute to the surface assembly. Two 25-pound cinder blocks were used to keep the surface assembly upright, and four blocks were used to lower and keep the parachute at the desired depth. Cinder blocks were found to have the following disadvantages: (1) a 50 percent weight loss in water requires that more blocks be used to keep the array vertical; and (2) with prolonged contact, the abrasive surface of the blocks tends to cut through the wire. Lengths of chain were looped through the blocks to prevent severing the wire.

At hourly intervals, the ship passed by each drogue and a Lorac navigational fix was taken; however, if the weather was good and the seas calm, one drogue was chosen as a reference point. A Lorac fix was taken at that drogue every hour, and radar ranges and bearings of the other drogues were taken from the fix. The drogues were tracked for periods up to 48 hours.

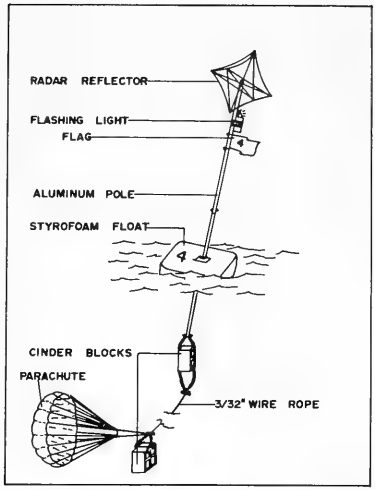

FIGURE 3. PARACHUTE-CURRENT DROGUE ASSEMBLY

4. Current Meter. Two Woods Hole Oceanographic Institution (WHOI) current meters (Model A-100), manufactured by the Geodyne Corporation, were used in an anchored array (Fig. 4). The meters operated for one lunar cycle of 28 days. The meter is a self-contained, digital recording instrument that measures current direction and speed (Geodyne Corporation, 1961).

5. Bottom Sediment. Kullenberg, PVC, and Phleger gravity corers were used for collecting bottom sediment samples. Short cores were designated as grab samples. The bottom samples were shipped to the NAVOCEANO geological laboratory for analysis.

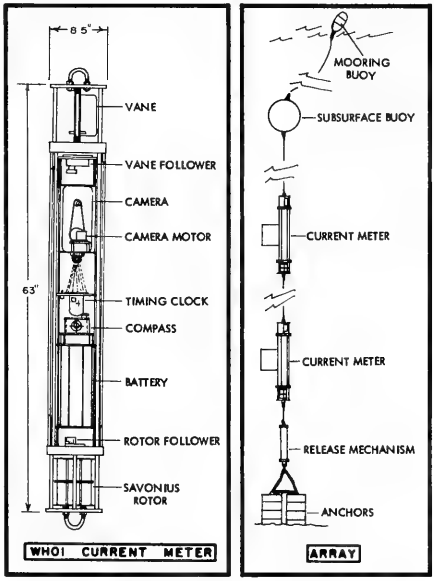

FIGURE 4. CURRENT METER AND ARRAY

6. Bottom Photography. Bottom photographs were taken using an Edgerton, Germeshausen, and Grier (EG&G) stereo camera system (Model 204 cameras, Model 214 light sources). A sonar pinger (EG&G Model 220) attached to the camera frame was used to position the array 3 to 5 meters off the bottom.

7. Plankton. Vertical plankton hauls were made using a 1-meter net. The maximum depth of a haul was determined by water depth, scattering layer depth, and sea conditions. The samples were preserved in an aqueous formaldehyde solution for later analysis at NAVOCEANO.

8. Bathythermograph. A mechanical 900-foot bathythermograph (BT) was used to obtain temperature versus depth profiles.

B. Data Processing and Presentation.

During survey operations, sound velocities were hand computed from Nansen cast data using tables developed from Wayne D. Wilson's equations of sound speed in sea water (NAVOCEANO, 1962) for comparison with velocimeter data. The velocimeter system gave a punch tape record of sound velocity, temperature, and depth. The tapes are on file at NAVOCEANO.

The Nansen cast data were checked, coded, and forwarded to the National Oceanographic Data Center (NODC) for computer processing. Machine listings provided temperature, salinity, dissolved oxygen, density (sigma-t), specific volume and dynamic depth anomalies, and sound velocity at standard depths. Listings of the Nansen cast data are on file at NODC under reference number 31935.

The parachute current data are presented in tabular form in the text under Currents. The film data records from the current meters were computer processed by Geodyne Corporation and forwarded to NAVOCEANO for analysis. A discussion and presentation of some of the current meter data also are found in the text under Currents.

The bottom sediment cores were analyzed at the NAVOCEANO geological laboratory for engineering properties and sediment size and composition. The grab samples were analyzed only for sediment size and composition. Core analysis summary sheets are on file at NAVOCEANO under Laboratory Item No. 277.

Representative photographs from each camera lowering are presented in the text under Bottom Photography. The film positives are on file at NAVOCEANO.

The plankton samples were sorted and identified at the NAVOCEANO biological laboratory. Qualitative and relative abundance analyses of the various plankters are presented in the text under Biological Analysis.

The BT slides were processed and the data are on file at NODC under reference number 06506.

Oceanographic parameters are reported in the English or metric units of measurement normal to the measuring instrument. For convenience, equivalents are given in figures and tables where applicable.

IV. PERSONNEL AND ACKNOWLEDGMENTS

Personnel participating in the survey were Messrs. R. A. Schaeffer (AGOR Coordinator), S. G. Tooma (Senior Scientist), H. Iredale, III, L. E. Jarvela, P. Bockman, and L. S. Jordan of NAVOCEANO, Mr. K. Hart of Seiscor Corporation, and Mr. R. K. Oser of the Geophysics Division, Pacific Missile Range.

Acknowledgment is given to Mr. R. A. Stewart for his interpretation of the geological data and Mr. J. A. Bruce for his distribution analysis of the biological data.

V. DATA ANALYSIS

A. Temperature.

Temperature-depth profiles of the oceanographic stations showed several interesting features. Representative profiles for both months are presented in Figure 5. In September, an isothermal layer extended to a depth of 15 meters. A sharp thermocline existed from this depth to about 150 meters below which temperatures decreased gradually to the lowest observed depth. The October data showed essentially the same distribution with the exception of the surface isothermal layer which was observed only to a depth of 5 meters.

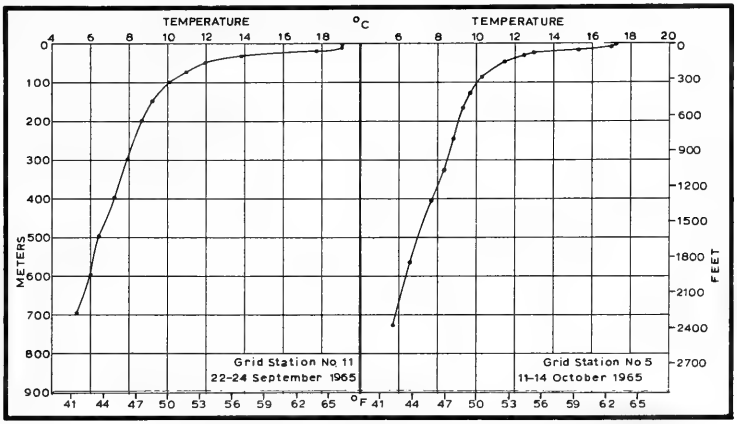

FIGURE 5. REPRESENTATIVE TEMPERATURE VERSUS DEPTH PROFILES

Two depths, 5 and 200 meters, were selected for presentation of horizontal temperature distributions (Fig. 6). The 5-meter depth

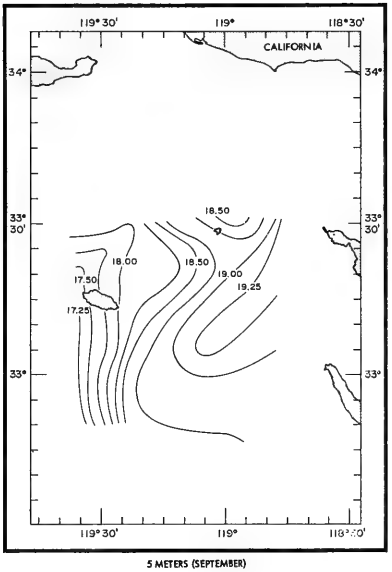

5 METERS (SEPTEMBER)

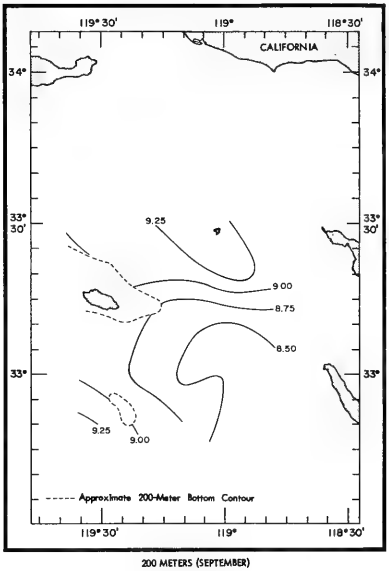

200 METERS (SEPTEMBER)

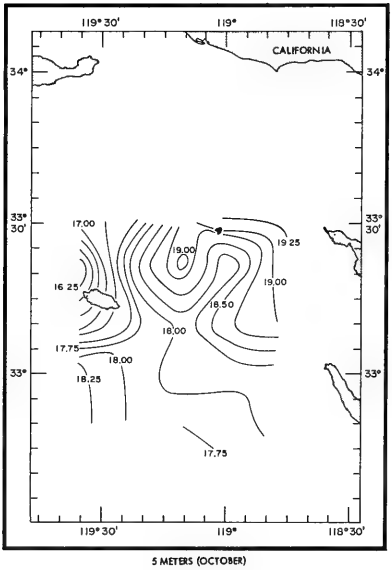

5 METERS (OCTOBER)

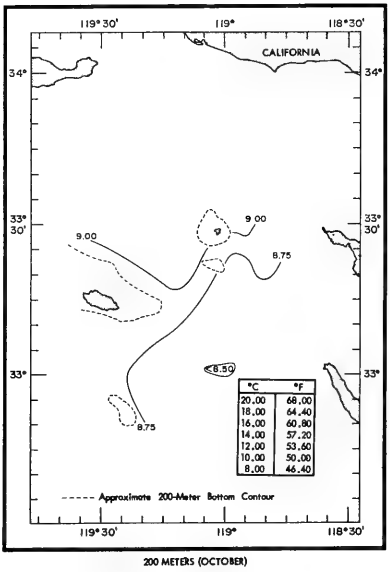

200 METERS (OCTOBER)

FIGURE 6. HORIZONTAL TEMPERATURE DISTRIBUTIONS

was selected to represent surface conditions, and the 200-meter depth was selected to represent subsurface conditions below the thermocline for the greatest number of stations.

In September, surface isotherms generally showed a north-south orientation with temperatures decreasing seaward. The 200-meter isotherms paralleled the bottom topography, and temperatures increased slightly in a northwesterly direction from the center of San Nicolas Basin.

During October, the surface isotherms indicated less north-south orientation than they did in September, but temperatures still decreased seaward. At 200 meters, the isotherms showed a similar orientation as in September, and temperatures increased from the center of the basin.

During both months, a sharp temperature gradient existed at the surface in the vicinity of San Nicolas Island, reflecting the effect of the California Current on the area. To the east, a tongue of warm water extended in a northeast-southwest direction.

B. Salinity.

Salinity-depth profiles indicated several recurring characteristics for the two operational periods. Figure 7 presents typical profiles representative of conditions observed in September and October. During September, an isohaline layer was observed to a depth of about 20 meters, a minimum at 30 meters, and an increase from 30 meters to the deepest observed depth. In October, the isohaline layer was observed to only 10 meters below which the profile resembled the September profile. **Salinity decreased about 0.2‰ from the isohaline layer to the minimum during both months.**

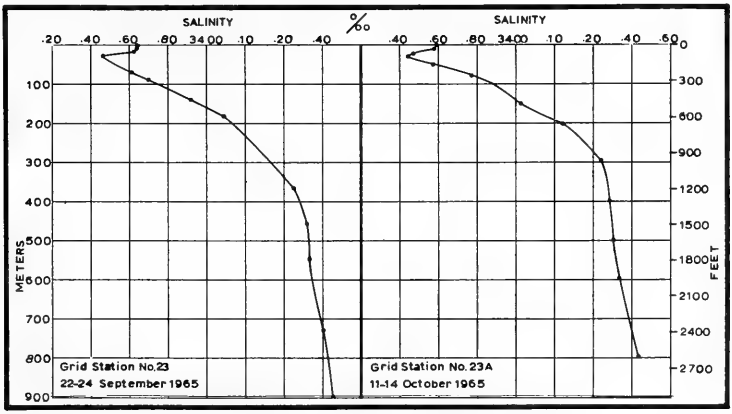

FIGURE 7. REPRESENTATIVE SALINITY VERSUS DEPTH PROFILES

Figure 8 shows horizontal salinity distributions at the surface

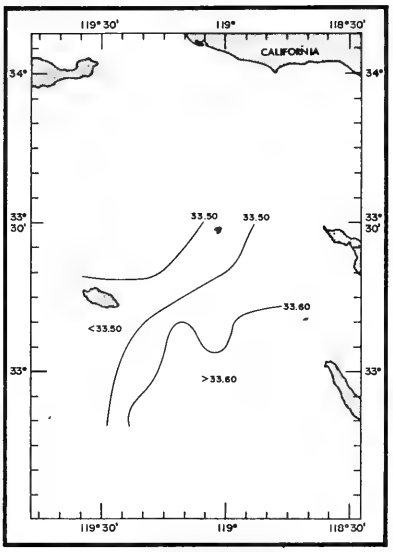

5 METERS (SEPTEMBER)

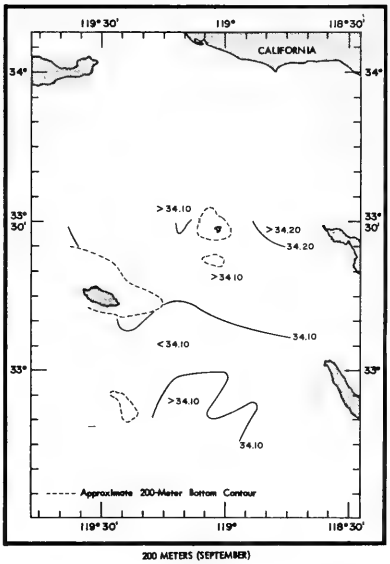

200 METERS (SEPTEMBER)

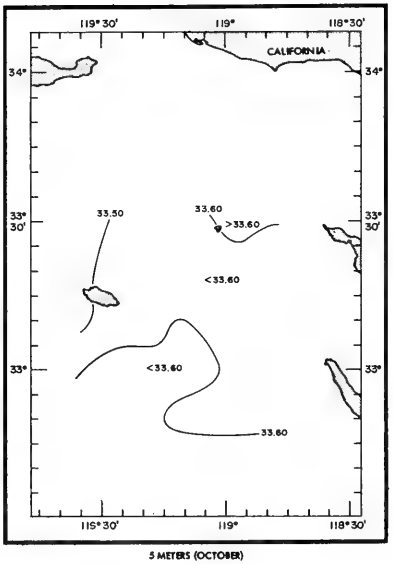

5 METERS (OCTOBER)

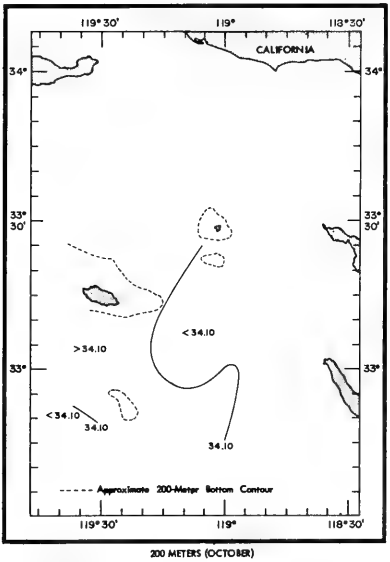

200 METERS (OCTOBER)

FIGURE 8. HORIZONTAL SALINITY DISTRIBUTIONS

and 200 meters for September and October. At both depths, salinities varied only about 0.2 ‰ . In September, surface salinities increased to the southeast with the isohalines oriented perpendicular to the California coast. At the surface in October, and at 200 meters for both months, salinities were slightly lower over the San Nicolas Basin, but they increased to the northeast and southwest. No significant orientation of isohalines is evident.

C. Dissolved Oxygen.

Dissolved oxygen determinations were made only on the September grid stations. In most cases, a mixed layer existed in the upper 15 meters. Below this layer, oxygen content increased sharply to a depth of 25 meters and then decreased steadily to a minimum at about 675 meters. A typical oxygen concentration profile is presented in Figure 9.

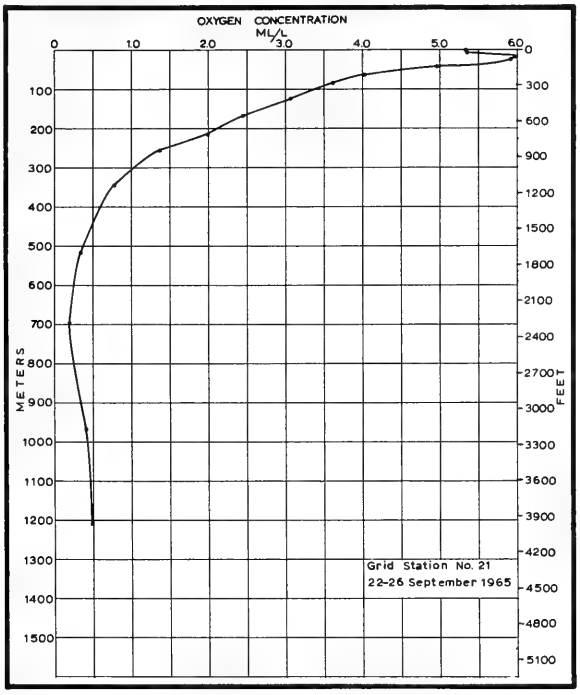

FIGURE 9. REPRESENTATIVE OXYGEN VERSUS DEPTH PROFILE

Horizontal distributions of oxygen at the surface and 200 meters are shown in Figure 10. North of San Nicolas Island, an area of lower dissolved oxygen concentration was observed at both depths.

This area was characterized by a much sharper gradient than in the surrounding waters with the decrease in concentration occurring in a northward direction.

Dissolved oxygen concentration averaged about 5.5 ml/1 at the surface and 2.0 ml/1 at 200 meters.

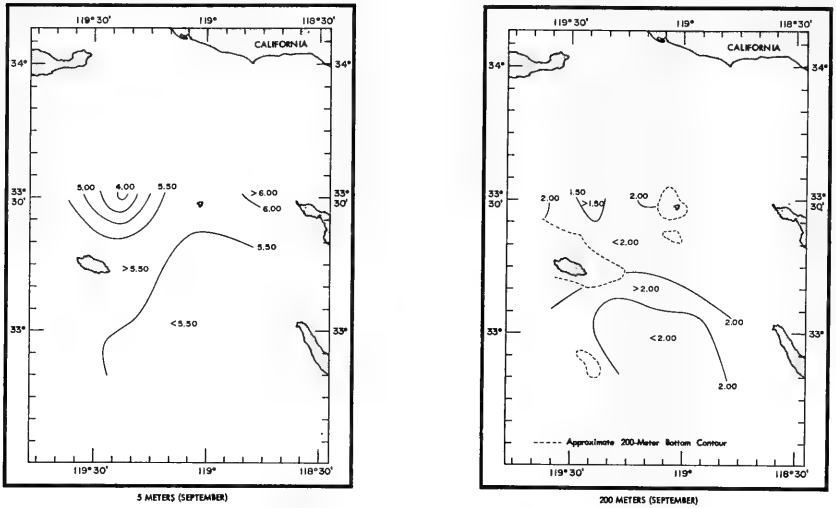

FIGURE 10. HORIZONTAL OXYGEN DISTRIBUTIONS

D. Sound Velocity.

1. Computed Sound Velocity from Nansen Cast Data. A representative sound velocity-depth profile is presented in Figure 11. This profile was drawn from data observed in October at station 19, located over the San Nicolas Basin. Sound velocity decreased sharply below 10 meters corresponding to the thermocline at the same depth. This decrease continued to approximately 100 meters where the gradient weakened. Although the October sound velocity values were slightly lower due to cooler temperatures, the profiles for both months were similar.

Axial depths remained almost constant at a depth of about 850 meters throughout both phases of the survey.

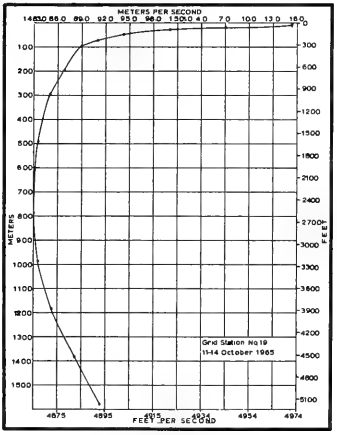

FIGURE 11. REPRESENTATIVE SOUND VELOCITY PROFILE FROM NANSEN CAST DATA

The sound channel was observed to be bottom bounded due to the shallow depths of the area. Surface duct development was usually restricted to the upper 10 meters and was observed most frequently in September.

At anchor stations, Nansen casts were taken primarily to investigate possible correlations between periodic sound velocity variations and the mixed tides characteristic of the Channel Islands area.

From the resulting data, the 24 to 28 hours allotted for these anchor stations appeared to be insufficient. A minimum of about 48 hours is necessary for a study of this type. Despite this drawback some definite trends were observed.

Figure 12 shows sound velocity variations at 400 meters for September anchor stations 1 and 2. The ordinate is exaggerated to illustrate more clearly the sinusoidal form of the curves. Sound velocities at 400 meters for the entire day had a range of 1.6 and 1.7 m/sec for stations 1 and 2, respectively. Comparing data from stations 1 and 2 at a particular hour, an estimated maximum difference of 1.2 m/sec occurred in the earlier part of the day. From 1400 to 2200 Zulu, the differences observed did not exceed 0.4 m/sec. Thus, the difference of values between the two stations at any hour is less than the range of values over the entire day for either station. This small difference of hourly sound velocities between the two stations is interesting considering that the two stations are approximately 19 miles apart, that San Nicolas Island lies between them, and that the stations were occupied on different days with some observations taken at different times.

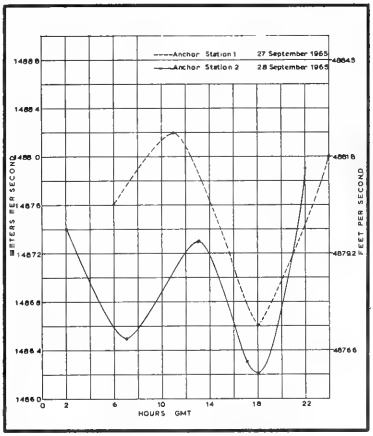

FIGURE 12. NANSEN CAST SOUND VELOCITY VERSUS TIME AT 400 METERS

2. Comparison of Nansen Cast and Ramsay Velocimeter Methods. Figure 13 shows the 400-meter sound velocity profile constructed from the Ramsay probe data at anchor station 1 in October. The sinusoidal curve also is evident; however, sound velocities were several meters per second greater than those derived from Nansen cast data. Figure 14 presents a comparison of sound velocities at 50 and 400 meters by the two methods for the same station. Difference in sound velocities, ΔV, was determined whenever a Nansen cast and a sound velocimeter lowering were made simultaneously. The average difference was slightly more than 3.4 m/sec. The curves, and especially ΔV, show the Ramsay probe values to be consistently higher than those derived from Nansen cast data. The most probable reason for this difference is an error in the multiplier or the zero

suppress settings of the AGODDS (AGOR Oceanographic Digital Data System) equipment. The settings of the AGODDS printout system are calibration constants which are used to convert the FM signals produced by the probe to usable values.

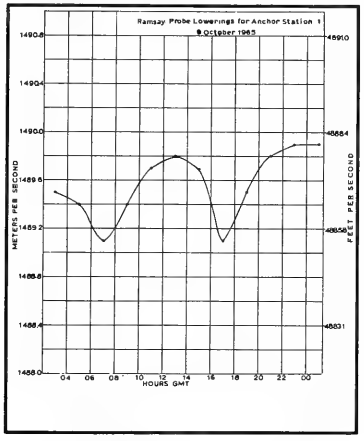

FIGURE 13. RAMSAY PROBE SOUND VELOCITY VERSUS TIME AT 400 METERS

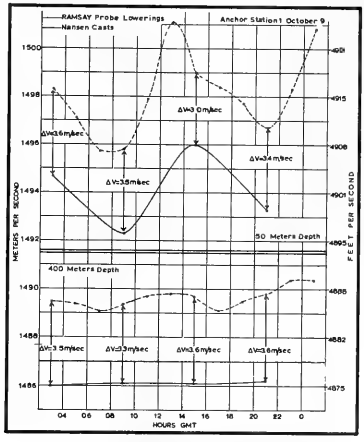

FIGURE 14. COMPARISON OF NANSEN CAST AND RAMSAY PROBE SOUND VELOCITIES

Despite the different values obtained by the two methods, the usefulness of a velocimeter is apparent. The velocimeter may be lowered repeatedly, is less time consuming, and gives more data points than do Nansen casts. The 50-meter profile in Figure 14 illustrates the difficulty of accurately determining maximum and minimum sound velocities during a 24-hour period using only four Nansen cast observations.

3. Discussion of Other Sound Velocity Influences. To explain the sinusoidal pattern of the sound velocity profiles, the tidal cycle was assumed to be the most influential factor. Figure 15 presents a set of representative time-series curves that were drawn from Nansen cast data at anchor station 1 (October) to possibly relate sound velocity variations with tides. The dashed curve in the middle of the figure represents observed tides at Los Angeles corrected for San Nicolas Island. At first glance, the high and low sound velocities appear to correspond to high and low tides, respectively. The similarity between the sound velocity profiles and the tidal curve is striking, especially at the 50-meter depth. This similarity is mainly the result of the ordinate scale employed and because

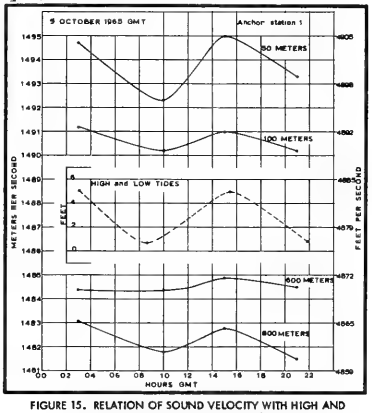

FIGURE 15. RELATION OF SOUND VELOCITY WITH HIGH AND LOW TIDES - ANCHOR STATION 1, OCTOBER

Nansen casts were coincidentally taken at about the time of high and low tides. A definite pattern, however, is indicated.

Using data collected on anchor station 2 (October), the same experiment was conducted to determine whether this pattern was a recurrent phenomenon. Resultant curves are shown in Figure 16. On this figure, Ramsay probe values were added after a 3.4 m/sec correction had been applied. Examination of these curves indicates that the peaks and troughs do not coincide as closely as those of anchor station 1. In fact, sound velocity maxima appear to be displaced to the right as the depth increases until maximum sound velocities correspond to low tide, a condition just the reverse of station 1.

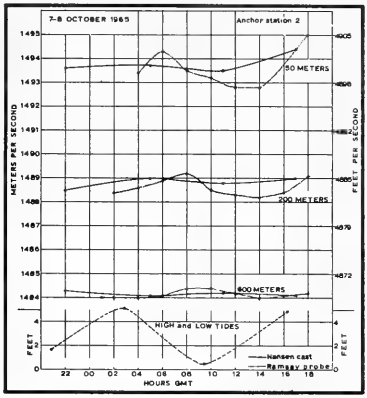

FIGURE 16. RELATION OF SOUND VELOCITY WITH HIGH AND LOW TIDES - ANCHOR STATION 2, OCTOBER

Sinusoidal oscillations of the Nansen cast sound velocity data were not as prominent at anchor station 1 as they were at anchor station 2. This result probably is due to the times at which the casts were taken, thus serving to illustrate the time requirement disadvantages of Nansen times for the different depths studied.

A comparison of data taken at anchor station 1 in both September and October revealed similar sinusoidal curves. Maximum and minimum velocities corresponded with high and low tides, respectively, but the September curves were not as pronounced as those in October. Anchor station 2 sound velocities did not display any relationships other than that maximum sound velocity values occurred at the same times for the different depths studied.

Another interesting feature at anchor station 1 (October) is the dampening of the sinusoidal pattern to mid-depth and the amplification at greater depths (Fig. 15). The 200- and 400-meter profiles, which are not presented in Figure 15, were nearly straight lines. At approximately 600 meters, the sinusoidal form once again becomes more obvious, and at 800 meters, the curve is similar to the one at 100 meters.

Anchor station 2 (October) did not display this increase in the range of sound velocity values at 600 meters, instead, dampening continued to the bottom. One explanation is that tidal forces have less effect as depth increases.

The differences between the two stations are difficult to explain. One possible solution could be the phases of the moon, but no connection seems likely as the time difference between occupation of anchor stations 1 and 2 in both September and October was only one day. Lunar phase effect on the tides could not possibly cause such a change

in 24 hours. The 10-day separation between the September and October measurements, however, could be another matter, but anchor station 1 showed this dampening both times and anchor station 2 neither time. The answer must be related to the station locations. Even though the stations are only 19 miles apart, they do have the San Nicolas Island ridge between them. The shallow depth of the ridge, about 55 meters, essentially isolates the two stations from each other. With the stations separated as they are, a phenomenon such as internal waves could affect one station and not the other. Defant (1950) stated that repeated Nansen casts in a single location have shown that vertical displacement of water masses does occur, and this has been related to internal waves. He also has shown that internal tide waves can exert a much greater influence on the thermohaline structure of the oceans than do normal tides. According to Sverdrup, et al (1942), the period lengths of such waves in many cases correspond to tidal periods. This could be the case at anchor station 1. Internal waves may not be caused by tide-producing forces but rather by periodic variations of actual tidal currents. Defant (1950) has concluded that the effects of the earth's rotation and internal waves are related and, together in varying combinations, may affect horizontal distribution of temperature, salinity, and sound velocity.

Further studies must be made of these interrelated parameters before any definite conclusions can be drawn. An increase in sampling frequency is needed as well. The use of a reliable and accurate sound velocimeter system fulfills this requirement.

E. Currents.

1. General. Water movement within the survey area was investigated in three ways: (1) parachute drogues, (2) self-recording current meters, and (3) dynamic computations.

2. Parachute Drogues. The drogue tracks at each of the five launch sites are presented individually in Figures 17 through 21. Also included in these figures are the tabular listings of drogue distance, time, and velocity for each interval between navigational fixes. The positions of navigational fixes are represented by circles which are connected by straight lines. Because of this method, computed speeds will be slightly less than the actual value. A few fixes appeared inconsistent with the data and were not used. This elimination of fixes also tends to give less drogue distance. Drag effect on the drogues, as discussed by Knauss (1963), was not taken into account due to shallow drogue depths.

Both average velocity and average interval velocity for each drogue track are presented in Table I. Average velocities were obtained by dividing the total distance covered by the drogue by the total amount of time used to cover the distance. The average interval velocity is the sum of the velocities for each interval between

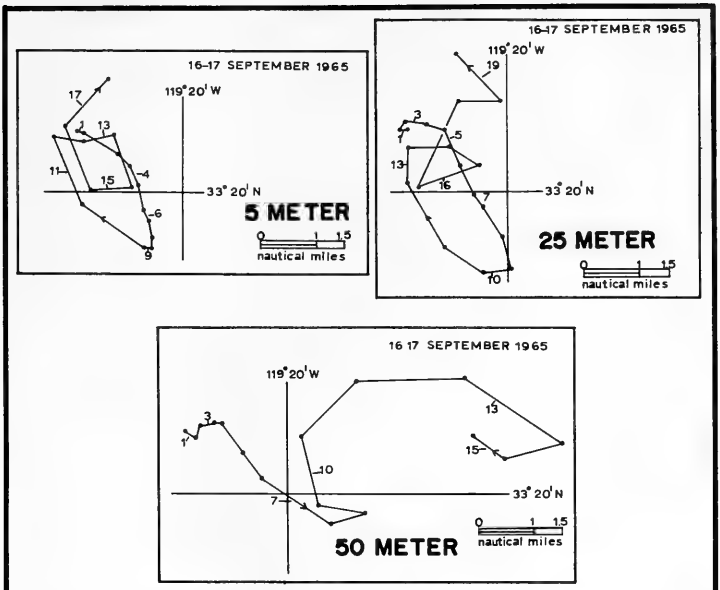

drogue depth	5 METER				25 METER				50 METER			
interval	distance naut mi	time hours	velocity kns	velocity cms/sec	distance naut mi	time hours	velocity kns	velocity cms/sec	distance naut mi	time hours	velocity kns	velocity cms/sec
1	.10	.75	.13	6.5	.12	.75	.16	8.0	.20	.63	.32	16.0
2	.76	1.55	.49	24.5	.17	.92	.18	9.0	.25	.92	.27	13.5
3	.22	.40	.55	27.5	.40	1.15	.35	16.5	.28	1.18	.24	12.0
4	.40	.90	.44	22.0	.31	.92	.34	17.0	.11	1.00	.11	5.5
5	.44	2.00	.22	11.0	.66	1.03	.64	32.0	.63	1.02	.62	32.0
6	.20	.27	.74	37.0	.61	.85	.72	36.0	.60	.88	.68	34.0
7	.32	1.18	.27	13.5	.20	.17	1.18	59.0	.93	1.53	.61	30.5
8	.20	1.77	.11	5.5	.66	1.20	.55	27.5	.50	1.33	.38	19.0
9	.16	1.08	.15	7.5	.57	1.35	.42	21.0	.63	1.57	.40	20.0
10	1.33	2.07	.64	32.0	.48	2.03	.24	12.0	.87	2.17	.40	20.0
11	1.30	2.22	.59	29.5	.80	1.45	.55	27.5	1.23	2.18	.56	28.0
12	.51	1.73	.29	14.5	1.28	1.98	.65	32.5	1.35	1.78	.76	38.0
13	.54	1.85	.29	14.5	.63	2.03	.31	15.5	1.83	2.00	.92	46.0
14	1.00	3.98	.25	12.5	.71	1.88	.38	19.0	2.05	2.67	.77	38.5
15	.80	2.37	.34	17.0	.62	2.57	.24	12.0	1.56	3.85	.41	20.5
16	1.24	3.10	.40	20.0	1.18	3.98	.30	15.0				
17	1.10	3.68	.30	15.0	1.71	3.13	.55	27.5				
18					.82	3.33	.25	12.5				
19					1.21	3.55	.34	17.0				

FIGURE 17. PARACHUTE DROGUE TRACKS – LAUNCH SITE 1

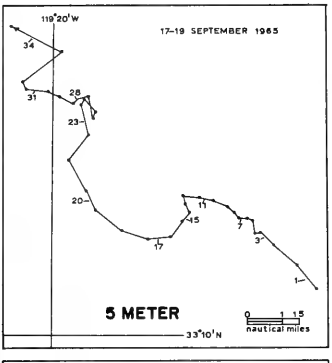

drogue depth	5 METER				25 METER			
interval	distance	time	velocity		distance	time	velocity	
	naut mi	hours	kns	cms sec	naut mi	hours	kns	cms sec
1	.96	1.57	.61	30.5	.50	1.58	.32	15.5
2	.83	2.32	.36	18.0	.24	2.22	.11	5.5
3	.53	1.12	.47	23.5	.61	1.12	.54	27.0
4	.15	.53	.28	14.0	.24	.53	.45	22.5
5	.32	.50	.64	32.0	.02	.50	.04	2.0
6	.20	.37	.54	27.0	.10	.37	.27	13.5
7	.19	.65	.29	14.5	.20	.65	.31	15.5
8	.24	.45	.53	26.5	.29	.45	.64	32.0
9	.26	.83	.31	15.5	.25	.83	.30	15.0
10	.47	1.00	.47	23.5	.50	1.00	.50	25.0
11	.40	1.00	.40	20.0	.33	1.00	.33	16.5
12	.48	1.20	.40	20.0	.24	1.20	.20	10.0
13	.25	.98	.26	13.0	.25	.98	.26	13.0
14	.24	.82	.29	14.5	.39	.82	.48	24.0
15	.37	1.00	.37	18.5	.23	1.00	.23	11.5
16	.71	1.00	.71	35.5	.32	1.00	.32	16.0
17	.65	1.00	.65	32.5	.31	1.00	.31	15.5
18	.80	1.00	.80	40.0	.21	1.00	.21	10.5
19	.97	1.00	.97	48.5	.40	1.00	.40	20.0
20	.59	1.00	.59	29.5	.32	1.00	.32	16.0
21	1.03	1.00	1.03	51.5	.41	1.00	.41	20.5
22	.88	1.00	.88	44.0	.18	1.00	.18	9.0
23	.91	1.00	.91	45.5	.11	1.00	.11	5.5
24	.12	1.92	.06	3.0	.19	1.90	.10	5.0
25	.38	1.17	.32	16.0	.22	.92	.24	12.0
26	.18	1.00	.18	9.0	.38	1.17	.32	16.0
27	.62	1.20	.35	17.5	.31	1.00	.31	15.5
28	.45	.88	.51	25.5	.62	1.20	.52	26.0
29	.38	1.02	.37	18.5	1.03	.88	1.17	58.5
30	.32	.98	.33	16.5	.23	1.02	.23	11.5
31	.62	1.07	.58	29.0	.27	.98	.28	14.0
32	.22	.85	.26	13.0	.38	1.07	.36	18.0
33	1.51	1.85	.82	41.0	.30	.85	.35	17.5
34	1.58	8.07	.20	10.0	.14	.97	.14	7.0
35					.32	1.78	.18	9.0
36					.31	1.05	.30	15.0
37					.30	1.28	.23	11.5
38					.66	1.38	.48	24.0
39					.39	1.62	.24	12.0

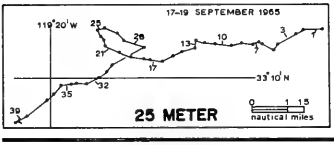

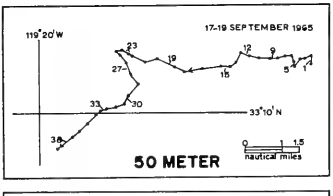

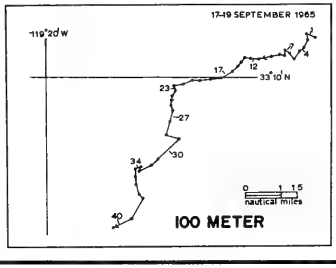

drogue depth	50 METER				100 METER			
interval	distance	time	velocity		distance	time	velocity	
	naut mi	hours	kns	cms sec	naut mi	hours	kns	cms sec
1	.27	1.40	.19	9.5	.21	1.30	.16	8.0
2	.22	2.17	.10	5.0	.13	.60	.22	11.0
3	.12	1.12	.11	5.5	.29	1.50	.19	9.5
4	.30	.53	.57	28.5	.17	1.12	.15	7.5
5	.23	.70	.46	23.0	.32	.53	.60	30.0
6	.16	.37	.43	21.5	.21	.50	.42	21.0
7	.20	.65	.31	15.5	.11	.37	.30	15.0
8	.17	.45	.38	19.0	.19	.65	.29	14.5
9	.22	.83	.27	13.5	.22	.45	.49	24.5
10	.37	1.00	.37	18.5	.21	.83	.25	12.5
11	.25	1.00	.25	12.5	.38	1.00	.38	19.0
12	.24	1.20	.20	10.0	.18	1.00	.18	9.0
13	.31	.98	.32	16.0	.20	1.20	.17	8.5
14	.21	.82	.26	13.0	.12	.98	.12	6.0
15	.21	1.00	.21	10.5	.11	.82	.13	6.5
16	.18	1.00	.18	9.0	.25	1.00	.25	12.5
17	.52	1.00	.52	26.0	.38	1.00	.38	19.0
18	.35	1.00	.35	17.5	.23	1.00	.23	11.5
19	.51	1.00	.51	25.5	.32	1.00	.32	16.0
20	.31	1.00	.31	15.5	.19	1.00	.19	9.5
21	.43	1.00	.43	21.5	.31	1.00	.31	15.5
22	.23	1.00	.23	11.5	.23	1.00	.23	11.5
23	.19	1.00	.19	9.5	.13	1.00	.13	6.5
24	.12	1.00	.12	6.0	.11	1.00	.11	5.5
25	.13	.83	.16	8.0	.24	1.00	.24	12.0
26	.28	1.17	.24	12.0	.21	.92	.23	11.5
27	.37	1.00	.37	18.5	.31	1.17	.26	13.0
28	.16	1.20	.13	6.5	.42	1.00	.42	21.0
29	.47	.88	.53	26.5	.39	1.20	.32	16.0
30	.25	1.02	.25	12.5	.81	.88	.92	46.0
31	.25	.98	.26	13.0	.15	1.02	.15	7.5
32	.29	1.07	.27	13.5	.41	.98	.42	21.0
33	.20	.85	.24	12.0	.11	1.07	.10	5.0
34	.11	.97	.11	5.5	.21	.85	.25	12.5
35	.43	1.78	.24	12.0	.20	.97	.21	10.5
36	.34	1.05	.32	16.0	.23	1.78	.13	6.5
37	.29	1.28	.23	11.5	.30	1.05	.29	14.5
38	.44	1.38	.32	16.0	.18	1.28	.14	7.0
39					.68	1.38	.49	24.5
40					.58	2.12	.27	13.5

FIGURE 18. PARACHUTE DROGUE TRACKS - LAUNCH SITE 2

drogue depth	5 METER			
interval	distance naut mi	time hours	velocity kns	velocity cms/sec
1	.14	.97	.14	7.0
2	.50	1.58	.32	16.0
3	1.79	5.48	.33	16.5
4	1.97	1.08	1.82	91.0
5	.37	.70	.53	26.5
6	.88	1.18	.75	37.5
7	.50	.90	.56	28.0
8	1.10	1.17	.94	47.0
9	.12	.73	.16	8.0
10	.20	1.25	.16	8.0
11	.15	.77	.19	9.5
12	.72	1.15	.63	31.5
13	.24	1.73	.14	7.0
14	1.31	.67	1.96	98.0
15	2.14	2.02	1.06	53.0
16	.47	.38	1.24	62.0
17	1.67	1.45	1.15	57.5
18	.44	.65	.68	34.0
19	1.02	1.23	.83	41.5
20	.61	.68	.90	45.0
21	1.14	.93	1.23	61.5
22	1.06	2.00	.53	26.5
23	1.15	1.77	.65	32.5
24	1.13	1.87	.60	30.0
25	.60	1.48	.41	20.5
26	.49	1.02	.48	24.0
27	.42	.82	.51	25.5
28	.78	1.28	.61	30.5
29	.33	.70	.47	23.5
30	.70	1.20	.58	29.0
31	.43	1.03	.42	21.0
32	.53	1.30	.41	20.5
33	.43	.90	.48	24.0
34	.62	1.67	.37	18.5
35	.73	1.05	.70	35.0
36	.51	.88	.58	29.0
37	.60	1.15	.52	26.0

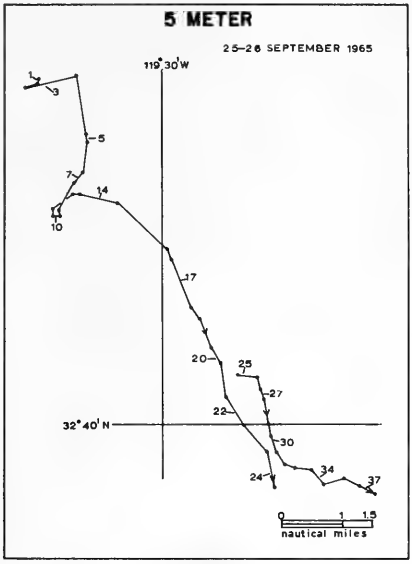

drogue depth	25 METER			
interval	distance naut mi	time hours	velocity kns	velocity cms/sec
1	.36	1.05	.34	17.0
2	.29	.75	.39	19.5
3	.48	2.13	.23	11.5
4	1.98	4.20	.47	23.5
5	.42	.67	.63	31.5
6	.65	1.27	.51	25.5
7	.10	.73	.14	7.0
8	1.15	1.48	.98	49.0
9	.25	.58	.43	21.5
10	.44	1.18	.37	18.5
11	.33	.78	.42	21.0
12	.10	1.27	.08	4.0
13	.21	.67	.31	15.5
14	.35	.72	.49	24.5
15	1.58	1.78	.89	44.5
16	.64	.75	.85	42.5
17	.62	1.00	.62	31.0
18	.83	1.08	.77	38.5
19	.57	.83	.69	34.5
20	.40	1.23	.33	16.5
21	.28	.52	.54	27.0
22	.80	2.93	.27	13.5
23	.64	1.50	.43	21.5
24	.57	.70	.81	40.5
25	.81	1.20	.68	34.0
26	.61	1.00	.61	30.5
27	.71	1.05	.68	34.0
28	.90	.98	.92	46.0
29	.62	1.05	.59	29.5
30	.41	.85	.48	24.0
31	1.08	1.40	.77	38.5
32	.61	.97	.63	31.5
33	2.64	1.57	1.68	84.0
34	.61	.90	.68	34.0
35	.91	3.77	.24	12.0

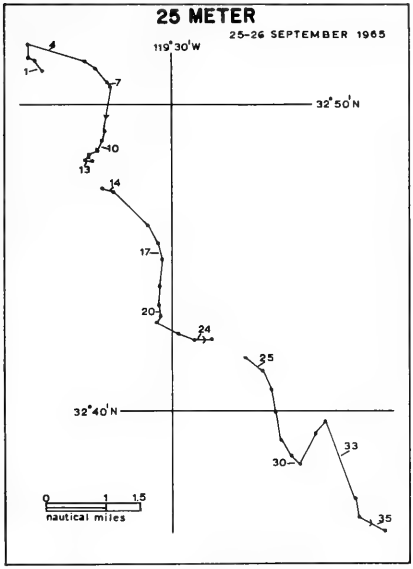

FIGURE 19. PARACHUTE DROGUE TRACKS – LAUNCH SITE 3

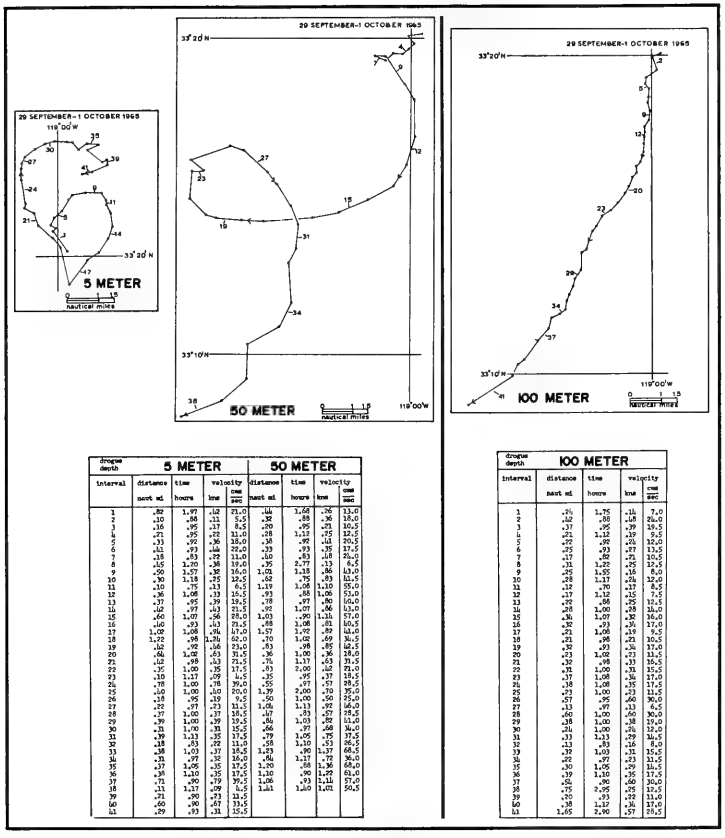

drogue depth	5 METER			50 METER		
interval	distance naut mi	time hours	velocity kns	distance naut mi	time hours	velocity kns
1	.09	1.97	.12	21.0	.44	1.68	.26	13.0
2	.10	.88	.11	5.5	.38	.88	.36	18.0
3	.16	.95	.17	8.5	.20	.95	.21	10.5
4	.21	.95	.22	11.0	.28	1.13	.25	12.5
5	.33	.92	.36	18.0	.38	.92	.41	20.5
6	.41	.93	.44	22.0	.33	.93	.35	17.5
7	.18	.93	.19	11.0	.10	.93	.11	5.5
8	.40	1.20	.33	16.0	.35	2.77	.13	6.5
9	.30	1.57	.19	16.0	1.02	1.18	.86	43.0
10	.30	1.18	.25	12.5	.62	.75	.83	41.5
11	.10	.75	.13	6.5	1.19	1.08	1.10	55.0
12	.36	1.08	.33	16.5	.93	.88	1.06	53.0
13	.17	.95	.19	10.5	.78	.97	.80	40.0
14	.42	.97	.43	21.5	.92	1.07	.86	43.0
15	.60	1.07	.56	28.0	1.03	.90	1.14	57.0
16	.40	.93	.43	21.5	.88	1.08	.81	40.5
17	1.09	1.08	.84	42.0	1.57	1.78	.89	44.0
18	1.72	.98	1.31	62.0	.70	1.02	.69	34.5
19	.62	.92	.66	33.0	.83	.98	.85	42.5
20	.66	1.02	.63	31.5	.36	1.00	.36	18.0
21	.42	.98	.43	21.5	.76	1.17	.63	31.5
22	.35	1.00	.35	17.5	.83	2.00	.42	21.0
23	.19	1.17	.16	8.0	.35	.95	.37	18.5
24	.78	1.00	.78	39.0	.55	.97	.57	28.5
25	.40	1.00	.40	20.0	1.39	2.00	.70	35.0
26	.18	.95	.19	9.5	.50	1.00	.50	25.0
27	.37	.97	.23	11.5	1.06	1.13	.92	46.0
28	.37	1.00	.37	18.5	.47	.93	.57	28.5
29	.39	1.00	.39	19.5	.84	1.03	.82	41.0
30	.31	1.00	.31	15.5	.66	.97	.68	34.0
31	.39	1.13	.35	17.5	.79	1.05	.75	37.5
32	.18	.93	.19	11.0	.58	1.10	.53	26.5
33	.38	1.03	.37	18.5	1.23	.90	1.37	68.5
34	.31	.97	.32	16.0	.84	1.17	.72	36.0
35	.37	1.05	.35	17.5	2.30	.88	1.36	68.0
36	.38	1.10	.35	17.5	1.30	.90	1.27	63.0
37	.71	.90	.79	39.5	1.06	.93	1.14	57.0
38	.11	1.17	.09	4.5	1.21	1.20	1.01	50.5
39	.21	.90	.23	11.5				
40	.60	.90	.67	33.5				
41	.29	.93	.31	15.5				

drogue depth	100 METER		
interval	distance naut mi	time hours	velocity kns
1	.04	1.75	.02
2	.62	.88	.70
3	.37	.95	.39
4	.21	1.12	.19
5	.22	.92	.24
6	.25	.93	.27
7	.17	.82	.21
8	.21	1.22	.17
9	.25	1.55	.16
10	.28	1.17	.24
11	.12	.70	.17
12	.17	1.12	.15
13	.22	.88	.25
14	.28	1.00	.28
15	.36	1.07	.32
16	.32	.93	.34
17	.21	1.08	.19
18	.21	.98	.21
19	.32	.93	.34
20	.23	1.02	.23
21	.22	.98	.23
22	.31	1.00	.31
23	.17	1.08	.16
24	.18	1.08	.17
25	.23	1.00	.23
26	.27	.95	.28
27	.13	.97	.13
28	.30	1.00	.30
29	.28	1.00	.28
30	.21	1.00	.21
31	.33	1.13	.29
32	.13	.93	.14
33	.32	1.03	.31
34	.22	.97	.23
35	.30	1.05	.29
36	.39	1.10	.36
37	.84	.90	.93
38	.25	2.95	.08
39	.20	.90	.22
40	.38	1.12	.34
41	1.65	2.90	.57

FIGURE 20. PARACHUTE DROGUE TRACKS – LAUNCH SITE 4

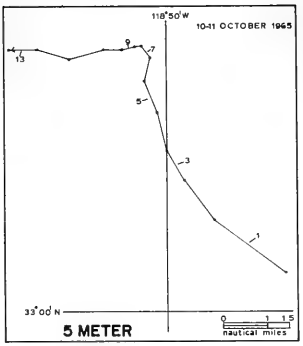

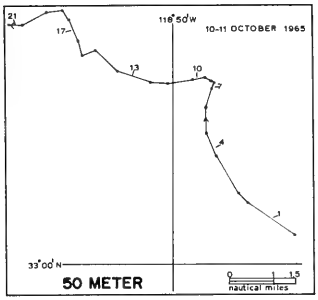

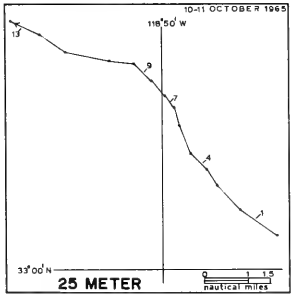

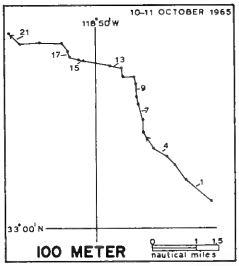

drogue depth	5 METER				25 METER			
interval	distance naut mi	time hours	velocity kms	velocity cms/sec	distance naut mi	time hours	velocity kms	velocity cms/sec
1	1.96	1.85	1.06	53.0	1.02	1.82	.56	28.0
2	1.07	1.08	.99	49.5	.70	1.08	.65	32.5
3	.77	.85	.91	45.5	.40	.85	.47	23.5
4	.82	1.07	.77	38.5	.52	1.07	.49	24.5
5	.68	1.02	.67	33.5	.67	1.02	.66	33.0
6	.59	.93	.63	31.5	.37	.93	.40	20.0
7	.31	.95	.33	16.5	.31	.95	.33	16.5
8	.11	.98	.11	5.5	.42	.98	.42	21.0
9	.34	1.17	.29	14.5	.53	1.17	.44	22.0
10	.41	.85	.48	24.0	.64	.85	.75	37.5
11	.74	1.25	.59	29.5	1.01	1.25	.81	40.5
12	.77	1.00	.77	38.5	.70	1.70	.70	35.0
13	.61	.85	.72	36.0	.64	.85	.75	37.5

drogue depth	50 METER				100 METER			
interval	distance naut mi	time hours	velocity kms	velocity cms/sec	distance naut mi	time hours	velocity kms	velocity cms/sec
1	1.20	1.78	.67	33.5	.71	1.72	.42	21.0
2	.32	1.07	.30	15.0	.36	1.07	.31	15.5
3	.90	.85	1.06	53.0	.79	.87	.33	16.5
4	.55	1.07	.51	25.5	.31	1.07	.29	14.5
5	.53	1.00	.52	26.0	.43	1.02	.40	20.0
6	.47	.93	.51	25.5	.31	.93	.33	16.5
7	.10	.95	.11	5.5	.29	.95	.31	15.5
8	.08	.98	.08	4.0	.16	.98	.16	8.0
9	.10	1.17	.09	4.5	.29	1.17	.25	12.5
10	.23	.85	.26	13.0	.15	.85	.18	9.0
11	.65	1.25	.52	26.0	.23	1.25	.18	9.0
12	.38	1.00	.38	19.0	.20	1.00	.20	10.0
13	.74	.85	.87	43.5	.28	.85	.33	16.5
14	.71	2.57	.28	14.0	.68	2.57	.26	13.0
15	.34	.30	1.13	56.5	.11	.30	.37	18.5
16	.35	1.02	.34	17.0	.17	1.02	.17	8.5
17	.48	1.05	.46	23.0	.17	1.05	.16	8.0
18	.23	.98	.23	11.5	.18	1.02	.18	9.0
19	.38	1.02	.38	19.0	.53	1.00	.53	26.5
20	.60	1.3	.59	29.5	.67	1.03	.66	33.0
21	.04	.	.30	15.0	.32	.95	.38	19.0

FIGURE 21. PARACHUTE DROGUE TRACKS - LAUNCH SITE 5

TABLE I. DROGUE VELOCITY SUMMARY

launch site	drogue depth meters	total distance nautical miles	total time hours	average velocity knots	average velocity cm/sec	average interval velocity knots	average interval velocity cm/sec
1	5	10.62	30.93	.34	17	.36	18
	25	13.14	34.28	.38	19	.44	22
	50	13.02	24.72	.53	26.5	.50	25
2	5	18.61	42.37	.44	22	.49	24.5
	25	13.10	40.42	.32	16	.36	18
	50	10.93	38.48	.28	14	.30	15
	100	10.66	40.52	.26	13	.28	14
3	5	27.99	46.82	.60	30	.65	32.5
	25	24.25	44.54	.54	27	.57	28.5
4	5	16.46	42.11	.39	19.5	.39	19.5
	50	29.10	43.29	.67	33.5	.71	35.5
	100	13.88	45.99	.30	15	.30	15
5	5	9.18	13.85	.66	33	.64	32
	25	7.90	13.82	.57	28.5	.57	28.5
	50	9.62	22.67	.42	21	.46	23
	100	6.60	22.67	.29	14.5	.29	14.5

navigational fixes divided by the total number of intervals. In this report, average interval velocity is used as the true water speed.

As shown in the drogue tracks, all 5-meter and most 25-meter drogues tended to rotate in a clockwise direction, usually in elliptical patterns. Good examples of this rotational effect can be seen in Figures 17 and 20. The deeper drogues, those at 50- and 100-meter levels, did not show as much rotational movement as those at 5 meters. They did move, however, in the same clockwise direction (Figs. 17 and 18). This rotation is a direct result of the tidal activity in the area.

At 5 meters, relatively slow current speeds were observed at the northernmost launch sites, 1 and 4. At the other three sites, drogue speeds at 5 meters were considerably faster. Drogue speeds at sites 1 and 4 were about 19 cm/sec. At site 2, slightly to the south, a speed of 24.5 cm/sec was observed, and at the southernmost sites, speeds were near 32 cm/sec.

At 25 meters, a flow similar to that at 5 meters was observed. The drogues launched at sites 1 and 2 moved at about 20 cm/sec, and speeds at the southernmost sites were greater than 23.5 cm/sec. The 25-meter drogue at site 4 lost its parachute before any usable data were obtained.

Conversely, the 50-meter drogues at the northernmost sites had the higher speeds. The water speed at site 1 was 25 cm/sec and at site 4 was 35.5 cm/sec. The latter speed was the highest observed. Speeds at sites 2 and 5 were 15 and 23 cm/sec, respectively. At site 3, the 50-meter drogue lost its parachute and was not recovered.

The lowest speeds (about 14 cm/sec) were found at 100 meters at sites 2, 4, and 5. No 100-meter drogue was released at site 1, and the one launched at site 3 was lost.

Generally, the drogue speeds at the three southern sites were highest at the surface and decreased with increasing depth. The drogue speeds at the northern sites were lower at the surface and increased with depth to 50 meters. Slow water speeds were observed at 5 and 100 meters at site 4, but a faster speed was indicated at 50 meters.

3. Current Meters. A current meter array was used for a lunar cycle of 28 days to relate current speed and direction, tides, and phases of the moon. A mooring site was selected 2 miles northeast of San Nicolas Island (Fig. 2). The array, illustrated in Figure 4, had the upper sensor at a depth of 30 meters and the lower sensor just above the bottom at 55 meters. Upon retrieval of the meters, the films were removed and sent to Geodyne Corporation for processing.

Three data presentation formats are presented in Figures 22 through 24. Figure 22 indicates the number of times a certain speed was observed during the 28-day cycle. Figure 23 shows direction and speed of current flow, in polar coordinates, and Figure 24 presents the same data in a scattergram.

Current velocities were computed by plotting compass and vane readings with speeds obtained from rotor readings. Velocity vectors for a 15-day period, covering the last-quarter and new moons, were summed in the x-y directions, and a resultant was obtained. At 30 meters, the overall velocity was 9 cm/sec at 122° True, and at 55 meters, the velocity was 7.5 cm/sec at 131° True.

Figures 25 and 26 present data obtained from the current meters. The figures show velocity components in the north-south and east-west directions, time of the particular phase of the moon, and computed tides. These figures also show relationships between speed and direction of the current, phases of the moon, and tides. Velocity components periodically cross the north-south and east-west zero vector lines, thus illustrating the rotational effect of tides on current direction.

The highest tides and greatest current speeds were found near the time of new moon. At that time, regular tides of uniform period and height variations and systematic current rotations were occurring. During full moon, tides were nearly regular, but not as high as those at new moon. Corresponding to this decrease in tide height was a lessening of current speed; rotation was rapid and systematic during this period. Irregular tides occurred at the first- and last-quarter moons.

The greatest dissimilarity between the current existing during the quarter moons and those of the new and full moons was that the current flowed in one direction for a much longer period of time during the quarter moons. Or, the current at the full- and new-moon periods rotated in a continuous clockwise direction; whereas, at the quarter-moon periods, the current oscillated between a clockwise and counterclockwise direction, not always completing a 360° rotation. Also, at the new- and full-moon periods, current flow rotated in a clockwise direction more consistently at 30 meters than near the bottom at 55 meters.

Based on the relationships discussed above, the following conclusions are made: (1) tides were regular a few days before until a few days after both the full and new moons; (2) tides were irregular a few days before until a few days after both the first- and last-quarter moons; (3) highest tides were found at the time of new-moon; (4) highest current velocities were found at new moon during the ebb; (5) currents rotated in a clockwise direction during new and full moons; (6) as depth increased, the trend of the current to rotate in a clockwise direction lessened; and (7) current direction alternated

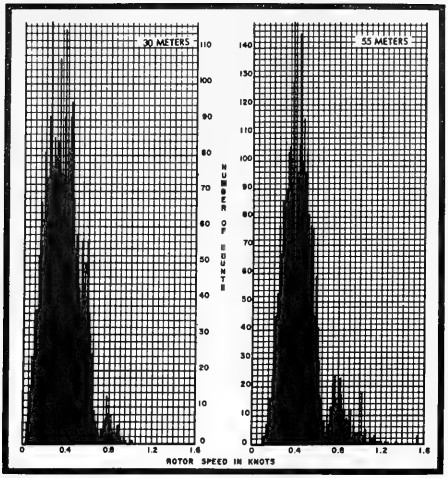

FIGURE 22. COUNTS VERSUS ROTOR SPEED FOR CURRENT METERS AT 30 AND 50 METERS

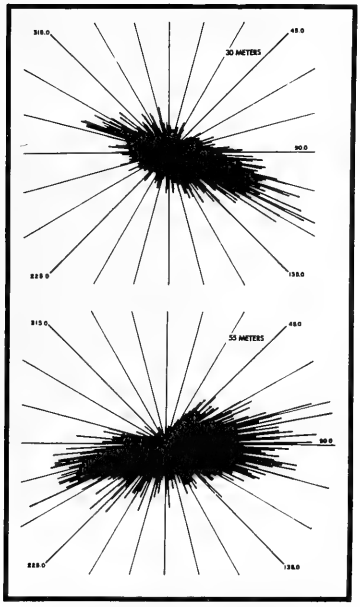

FIGURE 23. POLAR COORDINATE PLOTS FOR CURRENT METERS AT 30 AND 50 METERS

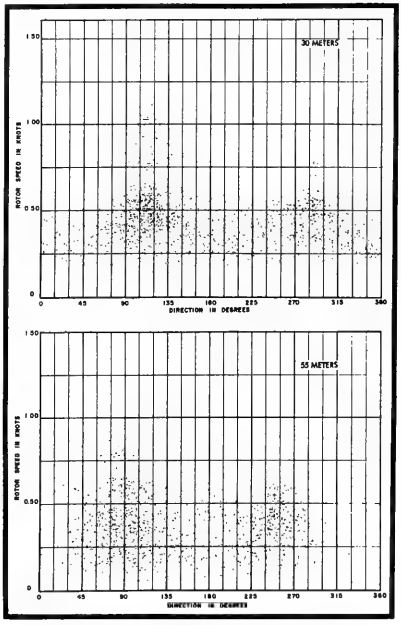

FIGURE 24. ROTOR SPEED VERSUS DIRECTION FOR CURRENT METERS AT 30 AND 50 METERS

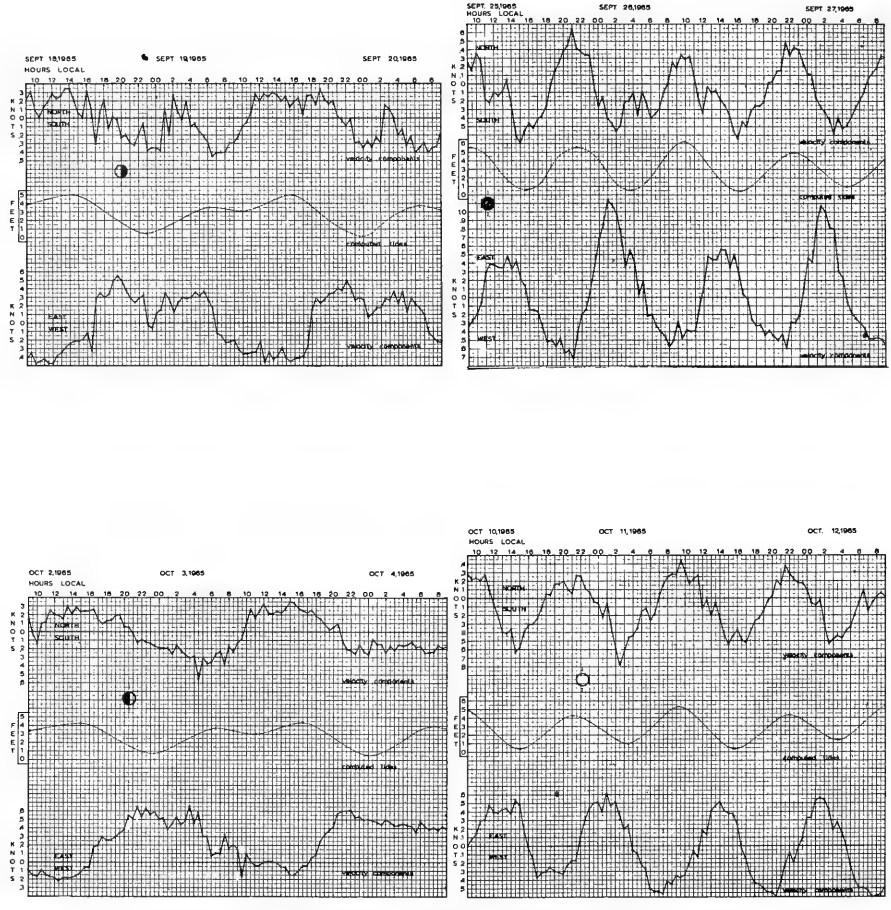

FIGURE 25. CURRENT METER VELOCITY COMPONENTS AT 30 METERS WITH COMPUTED TIDES FOR THE FOUR PHASES OF THE MOON

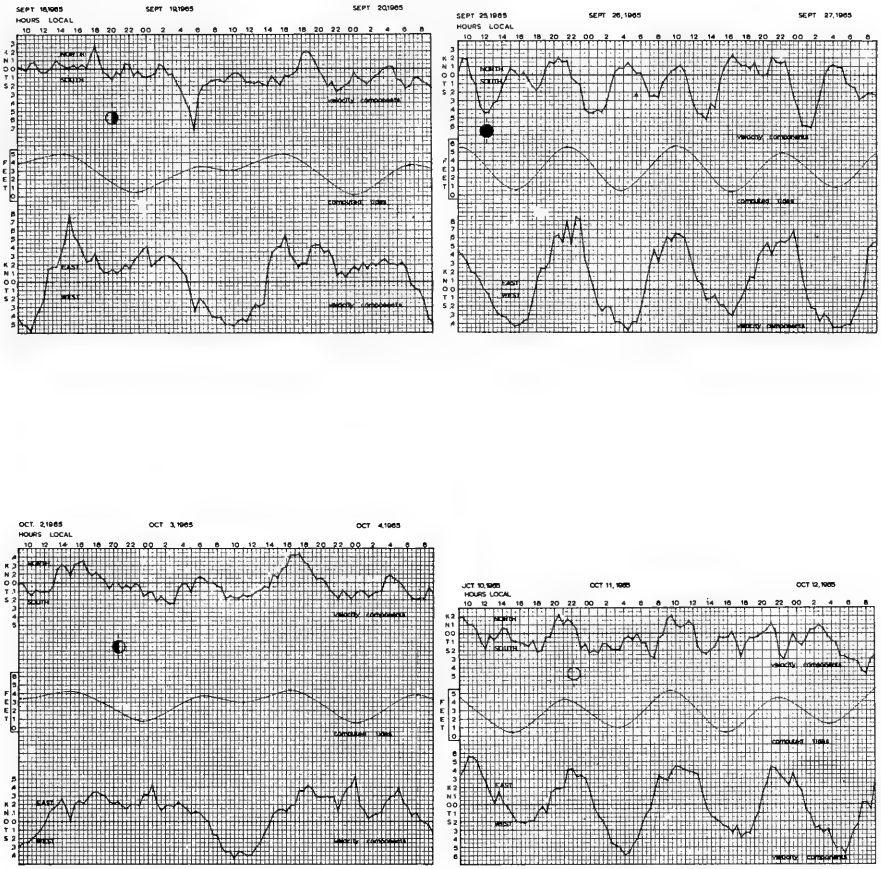

FIGURE 26. CURRENT METER VELOCITY COMPONENTS AT 55 METERS WITH COMPUTED TIDES FOR THE FOUR PHASES OF THE MOON

between clockwise and counterclockwise at both first- and last-quarter moons.

From (3) and (4) above, in the Channel Islands area the higher the tide, the faster the current speed. This point is further demonstrated because the lower tides of the full moon, as compared to the new moon, brought a correspondingly lower current speed. With increasing depth, the current meters were influenced less by the tides. From the upper current meter, data indicated that the current tended to rotate through 360° in a constant clockwise direction, whereas data from the lower current meter did not indicate a consistency in rotational direction. This rotational pattern was more apparent during the new and full moons when tidal activity was at a maximum.

4. Dynamic Topography. Dynamic height anomalies were derived and plotted primarily to supplement the results obtained by parachute drogue and current meter observations. The method for determining the reference level as outlined by Defant (1961) was used. In addition to the normal and well known limitations of this type of current analysis, three further variables for this survey are: (1) a study of a small area is subject to greater error than a large area (Sverdrup et al, 1942); (2) effects of the irregular coastline; and (3) varying depths (Reid et al, 1958). Despite these limitations, agreement with the parachute drogue results is exceptionally good. Using the September Nansen cast data, the 0-, 50-, and 100-decibar surfaces were contoured relative to the 500-decibar reference level (Fig. 27).

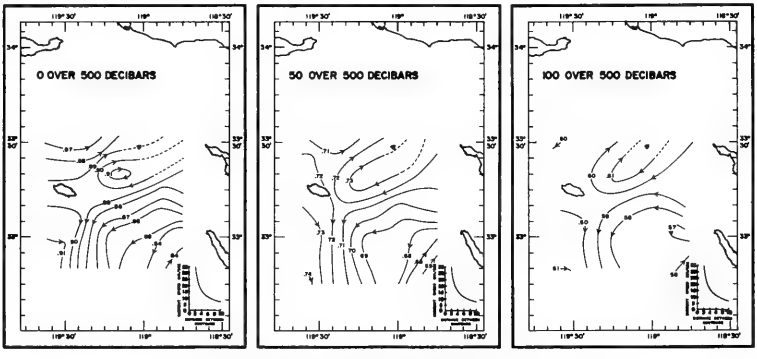

FIGURE 27. TOPOGRAPHY OF THE 0-, 50-, AND 100-DECIBAR SURFACES RELATIVE TO THE 500-DECIBAR SURFACE

The topographies depict a general counterclockwise flow around San Nicolas Basin with greater speeds at the periphery. Here, speeds of approximately 32.5 cm/sec were indicated at the 0-decibar surface which is in agreement with the 5-meter drogue released at site 3. In the water over the basin, drogue speeds decreased with increasing depth. Dynamic calculations also showed decreasing speeds with increasing depth.

The computed currents also agree well with results obtained by the current meters. The 50-decibar surface (Fig. 27) indicates a speed of approximately 22 cm/sec in the area of the current meter array. The histogram in Figure 22 shows that the current meter at 55 meters indicated a speed of approximately 22 cm/sec during most of its operation.

5. Summary of Water Circulation in the Channel Islands Area. The flow chart presented in Figure 28 was developed from data obtained by drogues, current meters, and dynamic calculations. Surface drogues which travelled in clockwise ellipses and did not show any appreciable displacement in any particular direction were not used in developing this chart.

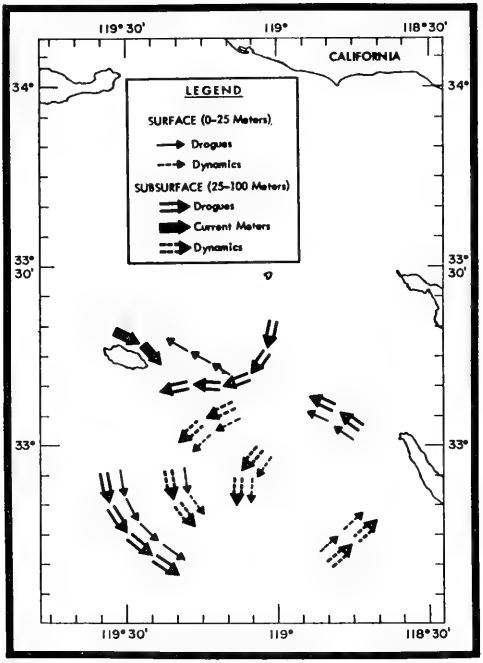

FIGURE 28. CIRCULATION PATTERNS FROM DROGUES, CURRENT METERS, AND DYNAMICS - SEPTEMBER AND OCTOBER 1965

The flow chart suggests an overall counterclockwise elliptical circulation that generally follows the bottom topography. This pattern has been presented in previous literature (For example, Horrer and Revelle, 1956). The flow chart also shows unidirectional flow of surface and subsurface waters with one exception in the area northeast of San Nicolas Island. Here, a small clockwise-moving gyre is formed

by the tides. Closer to the island, the current meter data indicated rotational water movement with a resultant vector to the southeast and a speed of 9 cm/sec.

Current meter data analysis indicated maximum clockwise rotation at new and full moons. Drogues, however, had maximum tidal rotation at the quarter moons which indicates that the drogues launched during the quarter moons (those at sites 1, 2, and 4) were launched in areas where localized eddies are formed by the tides. The drogues at sites 3 and 5 were launched when clockwise tidal rotation was at a maximum. The tidal forces were overpowered by the counterclockwise flow around the basin. Therefore, the speed of water flow around the periphery of the basin precludes the formation of tidal eddies. This result may not be true at the center of the basin where water speeds are not as great.

F. Bottom Composition.

1. Core Analysis. The area encompassed by this survey lies within the block-fault complex of deep basins and intervening sills, ridges, and banks that forms the sea floor off the southern California coast. As a result of concentrated work in this area over the past 20 years, the general characteristics of the bottom sediments are fairly well known. A comprehensive presentation of these characteristics and their significance is given by Emery (1960).

Basically, the sedimentary pattern is one of fine-grained sediments (chiefly silty clays) in the depressions and somewhat coarser material on the elevations. This basic pattern is presented only as a generalization, however, and variations may and do occur owing to several factors, the dominant of which is the mass downslope movement of sediment.

Sediments are supplied to the area from a variety of sources. Planktonic organisms, primarily foraminifera, are important contributors, and their importance increases with distance from shore. Fine terrigenous material is carried from the adjacent coast to the area by aerial and aqueous suspension. Subaerial erosion of exposed ridge tops (San Nicolas and Santa Barbara Islands) affords a proximate source of present day coarse and fine clastic detritus as did erosion of the more extensive ridges and banks during lower stages of sea level. Benthic organisms on shallow banks, island shelves, and ridges contribute abundant material, chiefly in the form of carbonate debris. Chemical precipitates, notably glauconite and phosphorite, may be important and even the dominant constituents on bank tops and ridge crests.

Sediment cores collected in the course of this survey (Fig. 2) generally support the known pattern. Samples from the Santa Cruz Basin (cores 2, 3, and 4), the San Nicolas Basin (cores 7, 8, 12, 13, 14, 15, 16, and 18; and grabs 9 and 10), and the Tanner Basin (core 17) were dominantly fine-grained, green-gray muds with rather

high organic content (up to about 9 percent). Occasionally, the cores were interfingered with lenses of increased sand content, especially those from areas adjacent to slopes. Carbonate content increased seaward from basin to basin, with the increasing importance of pelagic sedimentation in the form of foraminiferal tests. Carbonate values averaged from less than 30 percent of the total sediment in the Santa Cruz Basin to greater than 45 percent in the Tanner Basin. Cohesion values for the sediment surface (0 to 30 cm) were lowest in the Santa Cruz Basin (20 to 27 g/cm) and highest, for basin sediments in the San Nicolas Basin (75 to 82 g/cm) adjacent to the Santa Rosa-Cortes Ridge. (It should be noted that cohesion values obtained from these cores are questionable because 3 months lapsed before tests were made, and some desiccation had taken place.)

Sediments from the Santa Barbara Island slope (core 1 and grab 19) were greenish sandy muds. They represented a mixture of inorganic shelf sands and silts with coarser shelf fragments and small pelagic carbonate tests. The relative importance of organic remains was evident since carbonate values in excess of 40 percent were obtained. The greenish coloration of these sediments was due, at least in part, to the presence of glauconite and biotite grains. A strength test performed on core 1 resulted in a cohesion value of 44 g/cm .

The coarsest sediments obtained were from the San Clemente Ridge (cores 5 and 6) and the Santa Rosa-Cortes Ridge (core 11). These sediments may be classified texturally as sandy or gravelly muds and muddy sands. Composition of these ridge sediments may be highly variable depending on a specific locality. The coarse fractions may include any or all of the following particles: organic fragments, weathered rock fragments, mineral grains, or authigenic deposits. Carbonate content varies widely with the relative importance of the biogenic component. In line with the coarse character of the sediments, strength values obtained for the San Clemente Ridge sediments were high (about 237 g/cm). Core 11 was too short for reliable strength tests.

2. Bottom Photography. The distance covered on camera lowering numbers 1, 2, 3, and 4, was 0.7, 0.5, 1.0, and 0.4 nautical miles, respectively. In general, the bottom was uniform in composition throughout each drift track.

Camera lowering number 1 was taken on the San Nicolas slope toward the Santa Cruz Basin in 850 meters of water. A sequential series of six photographs from this lowering is presented in Figure 29. At the onset of the camera lowering, fine grained sediments associated with high organic debris dominated the area. Numerous animal tracks, echinoderm spines, and holes made by burrowing organisms can be seen. Approximately mid-way through lowering number 1, small nodules began to appear. Emery (1960) has shown the area covered by lowering number 1 to be a probable location of phosphorite nodules. This appears to

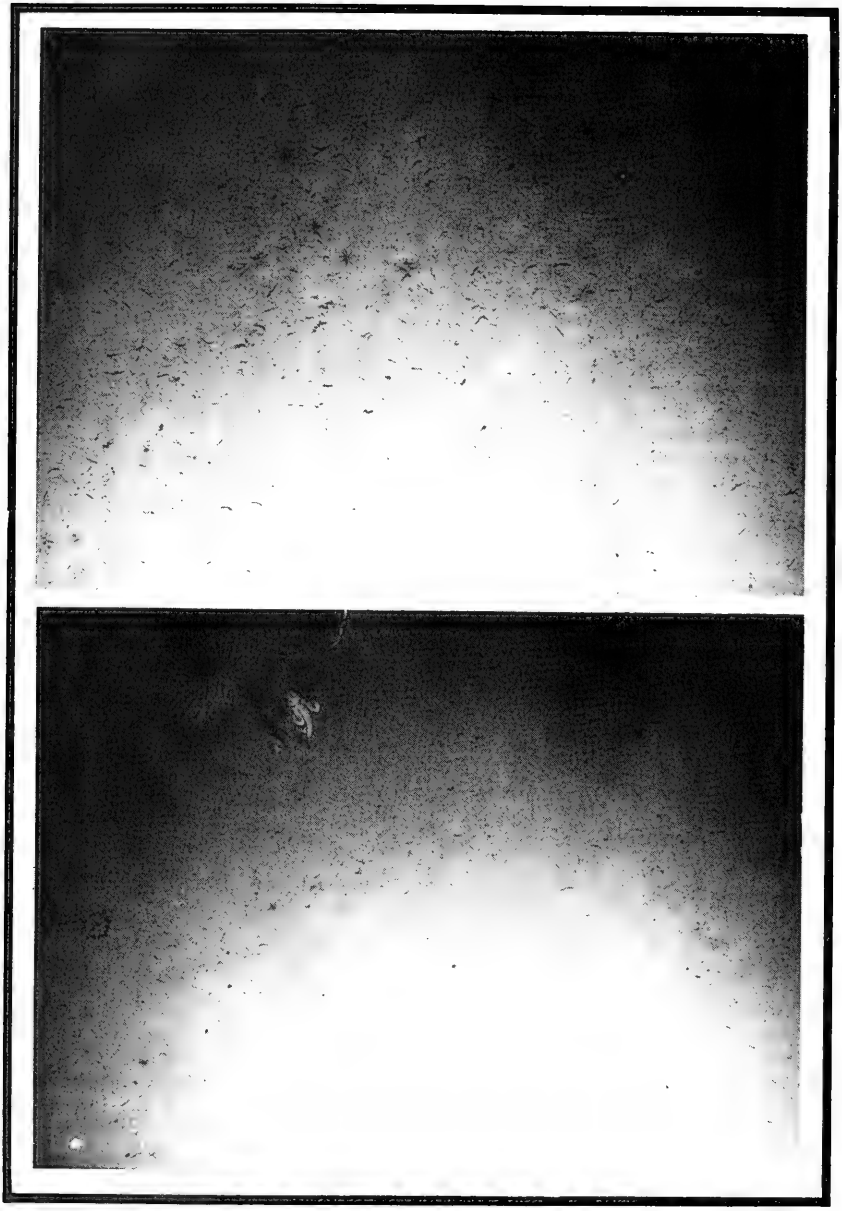

FIGURE 29. SEQUENTIAL SERIES OF BOTTOM PHOTOGRAPHS FROM CAMERA LOWERING NUMBER 1

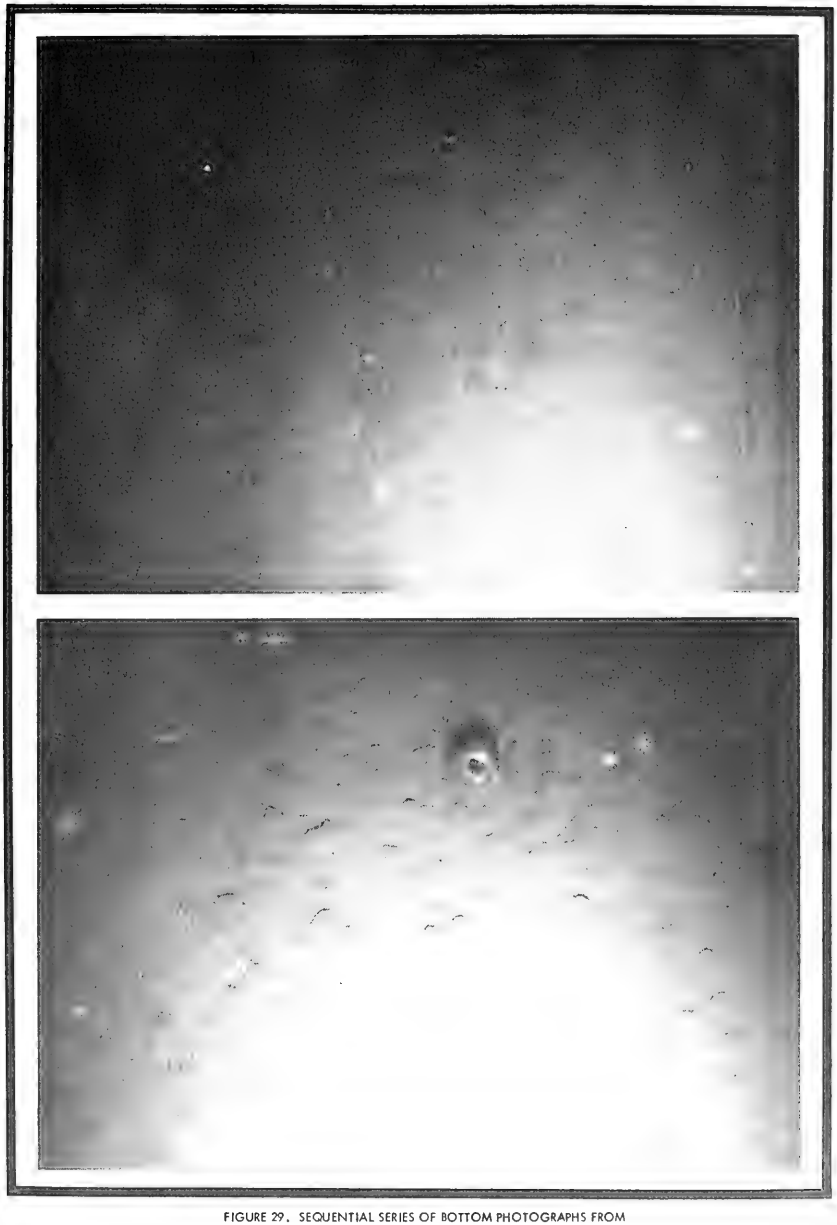

FIGURE 29. SEQUENTIAL SERIES OF BOTTOM PHOTOGRAPHS FROM CAMERA LOWERING NUMBER 1 (CONT'D)

FIGURE 29. SEQUENTIAL SERIES OF BOTTOM PHOTOGRAPHS FROM CAMERA LOWERING NUMBER 1 (CONT'D)

be the case. The concentration of these nodules increased to a maximum and then decreased until a very fine-grained muddy bottom prevailed.

Cores taken closest to the site of camera lowering number 1 were either in deeper water in the Santa Cruz Basin or in about the same depth as the camera lowering on the Santa Barbara slope. These cores were dominantly fine-grained, green-gray muds with high organic content.

Camera lowerings 2 and 3 were taken in the San Nicolas Basin in depths of 1100 and 1370 meters, respectively. Figures 30 and 31 present two photographs from each lowering. On both lowerings, fine-grained muds dominated the area. Numerous tracks and holes made by burrowing organisms can be seen. Biological activity shown in the lower photograph of Figure 30 illustrates the fine texture of the bottom. Brittle stars, observed throughout lowering number 3, are usually found in very fine-grained, soft, muddy bottoms. They feed on organic material which indicates this area to be one of high organic content.

Cores taken in the San Nicolas Basin substantiate the above observations. These cores, like the ones taken in the Santa Cruz Basin, were fine-grained, green-gray muds with a high organic content.

Camera lowering number 4 was taken on an elevation of the Santa Rosa-Cortes Ridge at a depth of 86 meters. The photographs taken on this lowering (Fig. 32) are not as clear as was desired. At this shallow depth, a large amount of particulate matter probably caused considerable diffusion of the strobe lights. The photographs from this lowering were dominated by in situ weathered rocks. The area appeared to be well-swept with bare bedrock visible in many photographs.

No cores were taken in the area of camera lowering 4, but cores taken on the San Clemente and Santa Rosa-Cortes Ridges were the coarsest obtained on this survey.

G. Biological Analysis.

Vertical plankton hauls were made with a 1-meter net of unknown mesh size while the ship was drifting on station (Fig. 2). Since the quantity of water that passed through the net is unknown, the population figures presented in the following paragraphs represent relative abundance of the various plankters rather than density per unit volume.

Plankton haul number 1 was taken on 23 September, 2 weeks before the other samples were collected. This haul, taken from a depth of 700 meters, was the second deepest haul made on the survey. A total of 55cc of plankton was obtained as compared to an average plankton volume of 16.8cc per haul obtained during October.

In a 3-week period between haul 1 and the October collection at

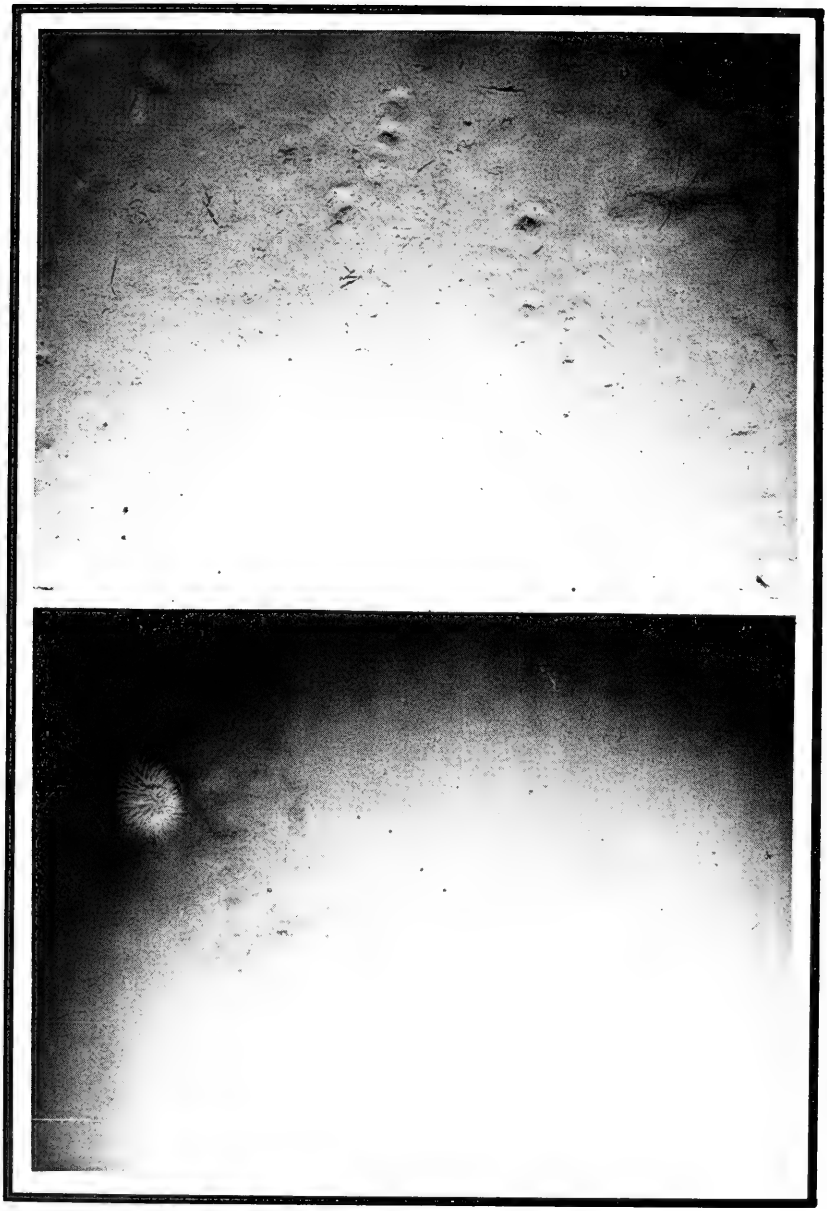

FIGURE 30. REPRESENTATIVE BOTTOM PHOTOGRAPHS FROM CAMERA LOWERING NUMBER 2

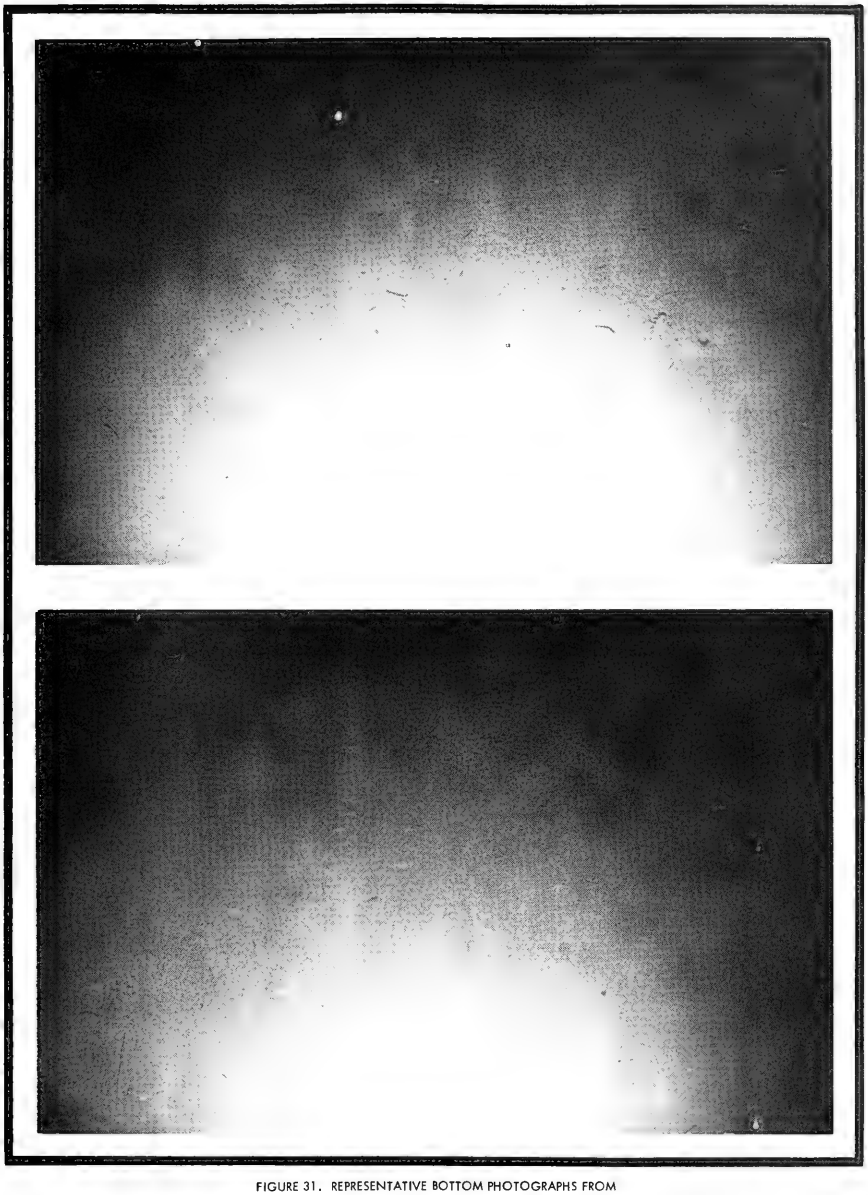

FIGURE 31. REPRESENTATIVE BOTTOM PHOTOGRAPHS FROM CAMERA LOWERING NUMBER 3

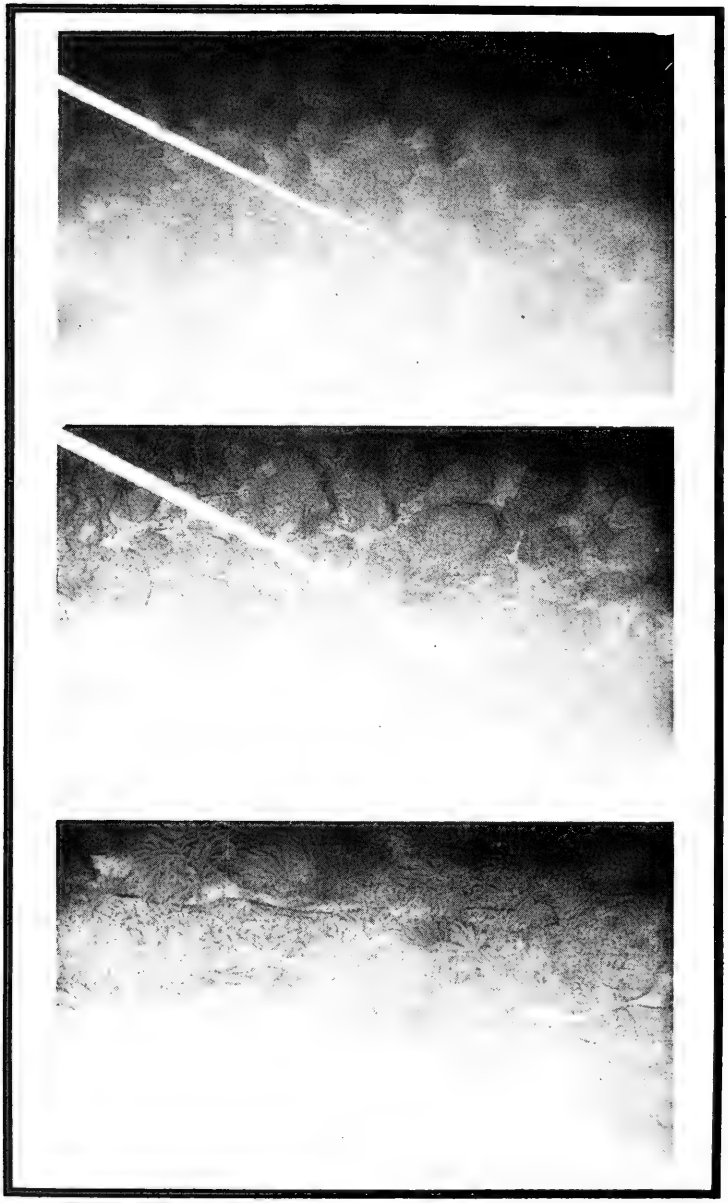

FIGURE 32. REPRESENTATIVE BOTTOM PHOTOGRAPHS FROM CAMERA LOWERING NUMBER 4

this location (haul 9), surface salinities varied about 0.1‰, and surface temperatures decreased by only 0.5°C. Nonetheless, there is a possibility that the survey area had less plankton volume in October than in September due to the autumnal decline.

Also in contrast to the October hauls, haul 1 contained several different species of copepods and amphipods as well as other different groups such as lamellibranchs (clams). Because of the varied nature of haul 1, only recognizable amphipods and copepods, composing about 71 percent of the total plankters, were classified to genus or species.

Haul 1 contained all but six of the 32 species of copepods obtained on the survey. The 26 species are listed below. Six of the species contained 88.2 percent of the total count of adult copepods. Immature copepods were much more numerous, but no attempt was made to estimate their numbers. Immature specimens of Corycaeus, sp., Oncaea sp., and Oithona sp. far exceeded the count of adults. Genera and families of known bioluminescence are marked with an asterisk; other genera here listed also may be bioluminescent.

Acartia sp.
Aegisthis
Candacia sp.
Calanus finmarchicus
Clausocalanus furcatus ┐ 66%
Clausocalanus arcuicornis ┘
Clymnestra sp.
*Corycaeus sp.
Euchaeta sp.
Euchirella sp.
Gaetanus pileatus
Gaetanus pungens
Haloptilis acutifrons
*Heterorhabdidae sp.
Lophothrix sp.
Lucicutia sp.
*Lucicutia flavicornis
*Metridia lucens 6%
*Microsetella sp.
Oithona sp.
Oncaea sp.
Pleuromamma sp. 7%
Rhincalanus cornutus 4.2%
Rhincalanus nasutus 5%
Scolecithrix sp.
Undeuchaeta major

The following amphipods occurred in small numbers in haul 1:

Acanthoscina acanthoides
Cyphocaris anonayx
Hyperia schizogeneics
Parathemisto pacifica
Paraphronima crassipes
Paraphronima gracilis
Hyperia n. sp.
Paraphonima sp.
Phronimopsis spinifera
Promno macropa
Scina crassipes
Vibilia armata
Vibilia (propinqua) sp.

Haul 11, taken from a depth of 1100 meters, was the deepest haul made. At least 22 species of copepods were present, of which the following differed from those obtained in haul 1:

Canadacia longimana
Euaugaptilus sp.
Eucalanus elongatus
Scolecithrix danae
Scolecithricella dentata
Scottocalanus securifrons

Of the four species of amphipods collected in haul 11, only Scina tulbergi is additional to the list from haul 1.

Figure 33 presents a series of plankton distributions for the October hauls. Because the September haul differed greatly from the October hauls, haul 1 was not used in drawing the distribution contours to avoid an unrealistic pattern. The plankton sample from haul 14 was damaged and was not analyzed. The first figure of the series presents the volume of plankton (wet volume in milliliters) collected at each station and the maximum depths sampled.

Specimens of the crustacea class were collected from all plankton stations. Copepoda, ostracoda, and euphausiaceae were in greater numbers than other crustacea and at all stations. Copepoda and ostracoda were most abundant in the eastern part of the survey area, whereas euphausiaceae were more abundant in the northern and southern parts. The distribution figures for cirripedia larvae, cladocera, amphipoda, and decapoda larvae show that these crustacea were not collected at all stations. Cirripedia (barnacle) larvae were more abundant over the San Nicolas Basin than in the shallow waters where they might normally be expected to attach. Cladocera were most numerous in the northeastern and southwestern parts of the survey area, and amphipoda were most numerous in the eastern portion. Decapoda were not collected from two of the easternmost stations. The greatest abundance was north and southeast of San Nicolas Island.

Small medusae (jellyfish) were unusually numerous with greatest concentrations over the deeper parts of the San Nicolas and Santa Cruz Basins. Siphonophora (colonial jellyfish) were more numerous in the eastern part of the survey area.

Bryozoan larvae were found to be most abundant at the easternmost stations in the area. Foraminifera were also found most abundant at the easternmost stations, but none were collected at the two northernmost stations.

Gastropod larvae were concentrated over the northern slope of San Nicolas Island toward the Santa Cruz Basin and at the southeastern-most station over the San Nicolas Basin. Counts decreased to zero intermediately between these two points. Pteropoda were concentrated on haul number 7, southeast of Santa Barbara Island, where no gastropod larvae were collected.

Larvaceae were most abundant at stations around the periphery of the survey area. The greatest concentration of Thaliacea (salps) was on haul number 4 over the Santa Cruz Basin. None were collected on haul number 7.

Chaetognatha were found at all stations but were centered in two areas of abundance, one over the center of the San Nicolas Basin

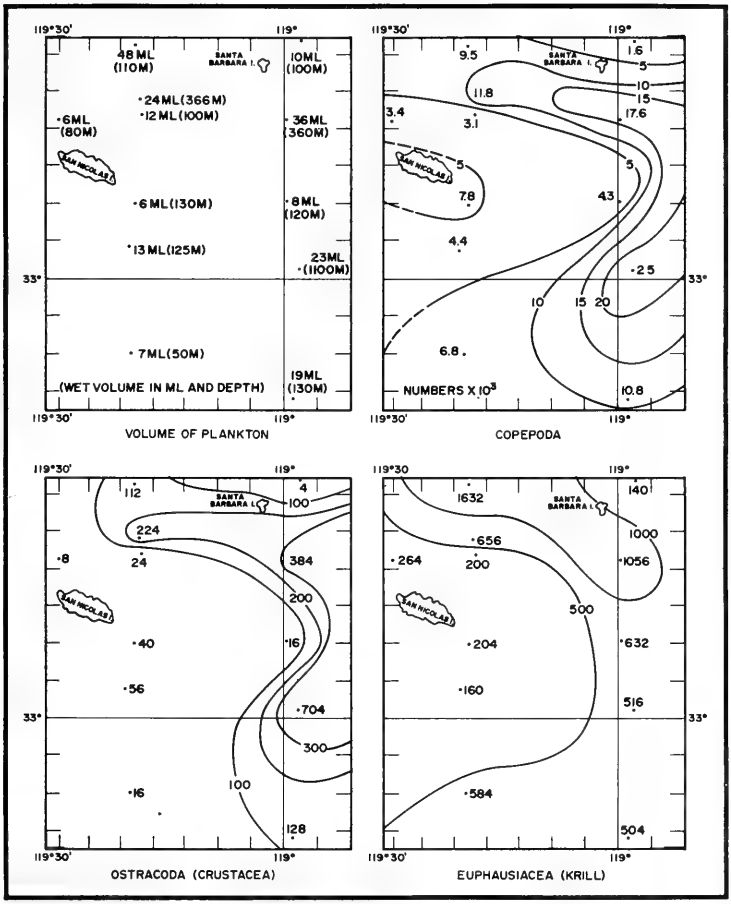

FIGURE 33. PLANKTON DISTRIBUTION

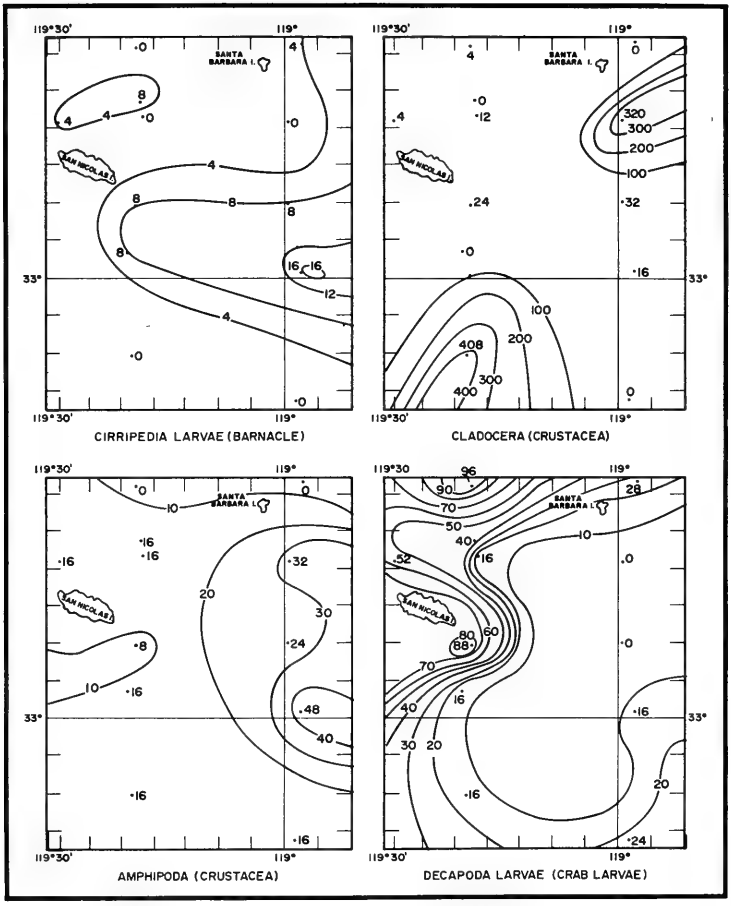

FIGURE 33. PLANKTON DISTRIBUTION (CONT'D)

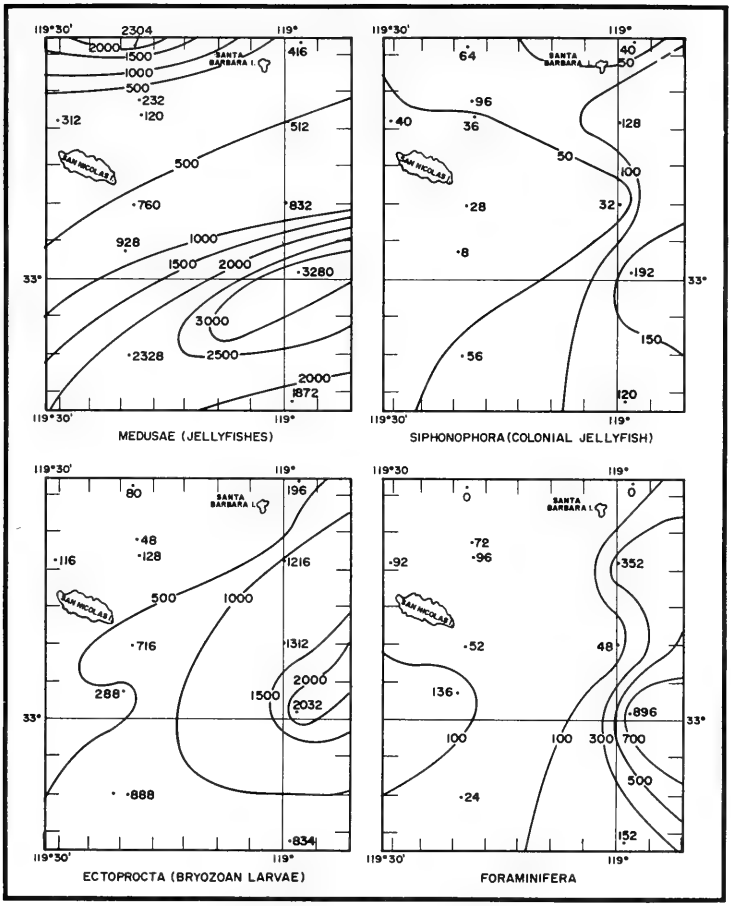

FIGURE 33. PLANKTON DISTRIBUTION (CONT'D)

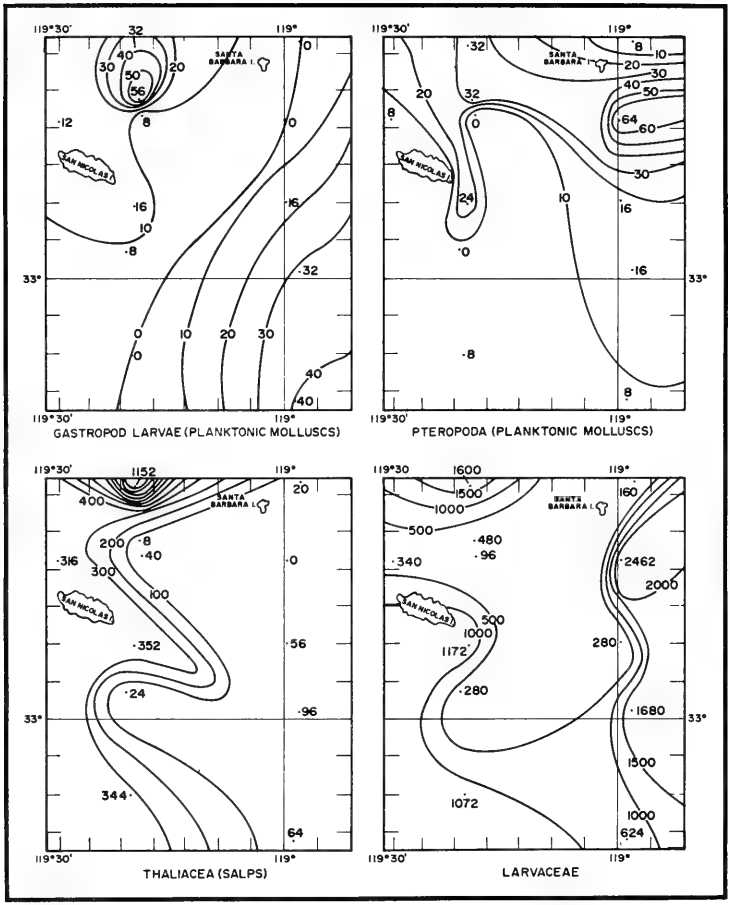

FIGURE 33. PLANKTON DISTRIBUTION (CONT'D)

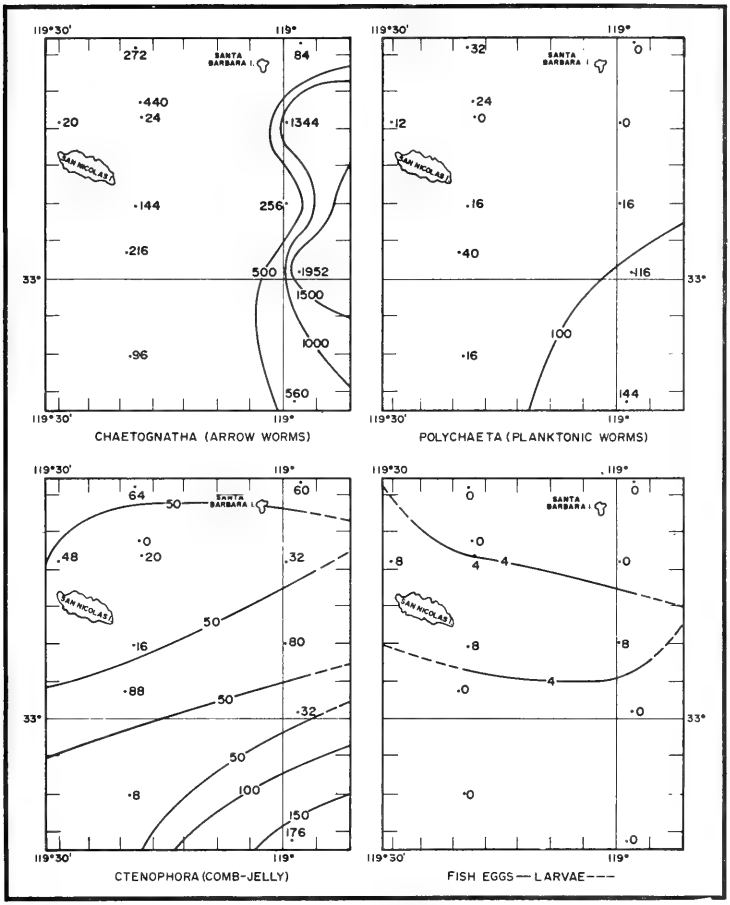

FIGURE 33. PLANKTON DISTRIBUTION (CONT'D)

and the other southeast of Santa Barbara Island. Polychaeta and Ctenophora were most numerous in the southeastern part of the survey area, and they were not collected at all stations.

The small number of fish eggs collected were distributed over four of the stations in the center of the survey area. Fish larvae were collected on haul number 8 only.

VI. SUMMARY AND CONCLUSIONS

The cold, low salinity California Current resulted in seaward decreases in surface temperatures and salinities. During both the September and October operational periods, a sharp temperature gradient existed at the surface in the vicinity of San Nicolas Island. In September, a mixed layer existed to a depth of about 20 meters, but in October, the mixed layer was only to 10 meters.

Dissolved oxygen determinations were made on the September stations. A mixed layer of dissolved oxygen generally occurred in the upper 15 meters. Dissolved oxygen concentration averaged about 5.5 ml/l at the surface and about 2.0 ml/l at 200 meters (656 feet). Minimum concentrations existed at about 675 meters (2215 feet).

The sound channel was bottom bounded due to the shallow depths of the survey area, and the sound velocity axis occurred at a depth of 850 meters (2800 feet). Surface duct development was usually restricted to the upper 10 meters and was observed most frequently in September.

At two 24-hour anchor stations, Nansen cast and sound velocimeter data showed temperatures, salinities, and sound velocities to oscillate in a sinusoidal manner throughout a day. At one of the anchor stations, maximum and minimum sound velocities corresponded with high and low tides, respectively. At the second anchor station, this situation was nearly the reverse. An explanation for this variation was the separation of the two anchor stations by San Nicolas Island and the effects of the earth's rotation and internal waves acting together in varying combinations at the stations.

Current data from parachute current drogues, current meters, and computed dynamics showed the San Nicolas Basin to be the center of a counterclockwise elliptical circulation. A unidirectional flow of surface and subsurface waters existed in the survey area with one exception in the area northeast of San Nicolas Island. Drogues and dynamic computations showed maximum current speeds of about 25 cm/sec around the periphery of San Nicolas Basin. Lesser speeds existed towards the center of the basin and with increasing depth. Current meters indicated an overall clockwise rotational tidal current to exist 2 miles northeast of San Nicolas Island. A resultant east-southeasterly flow of about 8 cm/sec was derived from the current

meter data. These data also indicated currents to be greatest at the new and full moon periods, especially during the tidal ebb.

Sediment samples from Santa Cruz, San Nicolas, and Tanner Basins were dominantly fine-grained, green-gray muds with rather high organic content. Sediments from the Santa Barbara Island slope were greenish sandy muds. They represented a mixture of inorganic shelf sands and silts with coarser shelf fragments and small pelagic carbonate tests. The coarsest sediments obtained were from the San Clemente Ridge and the Santa Rosa-Cortes Ridge. These sediments may be classified texturally as sandy or gravelly muds and muddy sands.

From one plankton collection in September and 13 in October, a study of the abundance of various plankters suggested that the autumnal decline occurred between 23 October September and the second week of October.

VII. BIBLIOGRAPHY

Carlson, Q., 1962. Digital Vibrotron Techniques. IMR 10-62. Unpublished Manuscript. U.S. Naval Oceanographic Office, Washington, D.C.

Defant, A., 1950. On the Origin of Internal Tide Waves in the Open Sea. J. Mar. Res. Vol. 9, No. 2, Sears Foundation for Marine Research, New Haven, pp. 111-119.

_____, 1961. Physical Oceanography. Pergamon Press, Vol. 1, New York, pp. 492-512.

Emery, K. O., 1956. Deep Standing Internal Waves in California Basins. The American Society of Limnology and Oceanography. Vol. 1, No. 1, pp. 35-41.

_____, 1960. The Sea Off Southern California; A Modern Habitat of Petroleum. John Wiley & Sons, Inc., New York.

_____, and Rittenberg, S. C., 1952. Early Diagenesis of California Basin Sediments in Relation to Origin of Oil. Bulletin of the American Association of Petroleum Geologists. Vol. 36, No. 5, American Association of Petroleum Geologists, Ann Arbor, pp. 735-804.

Geodyne Corporation, 1961. Instruction Manual A-100 Current Meter. Waltham, Mass.

Gorsline, D. S., 1966. Continental Borderlands, Rhodes W. Fairbridge, ed. Encyclopedia of Oceanography, Reinhold Publishing Corporation, New York, pp. 197-200.

Horrer, P. and Revelle, R., 1956. The Oceans Off the California Coast. Scripps Institution of Oceanography - Contributions 1956, pp. 429-446.

Knauss, J. A., 1963. Drogues and Neutral-Buoyant Floats, M. N. Hill, ed. The Sea. Interscience Publishers, New York, pp. 303-304.

LaFond, E. C., 1951. Processing Oceanographic Data. H.O. Pub. 614, U.S. Navy Hydrographic Office, Washington, D.C., pp. 16-19.

MacGinitie, G. E. and MacGinitie, N., 1949. Natural History of Marine Animals. McGraw Hill, Inc., New York.

Marmer, H. A., 1926. Coastal Currents Along the Pacific Coast of the United States. Government Printing Office, Washington, D.C.

Menard, H. W., 1964. Marine Geology of the Pacific. McGraw-Hill, Inc., New York, pp. 171-190.

Reid, J. L., 1962. Measurements of the California Countercurrent at a Depth of 250 Meters. J. Mar. Res. Vol. 20, No. 2, Sears Foundation for Marine Research, New Haven, pp. 584-602.

_____, Roden, G. I., and Wyllie, J. G., 1958. Studies of the California Current System In Cal. Dept. Fish and Game, Marine Research Committee, Calif. Coop. Oceanic Fish. Invest., Prog. Rep. 1 July 1956 - 1 Jan. 1958, pp. 27-56.

Ricketts, E. F., and Calvin, J. V., 1964. Between Pacific Tides. Stanford University Press, Stanford, California.

Sverdrup, H. U., and Fleming, R. H., 1937. The Waters Off the Coast of Southern California - March to July 1937. Bulletin of Scripps Institution of Oceanography. Vol. 4, No. 10, LaJolla, pp. 261-378.

Sverdrup, H. U., Johnson, M. W., and Fleming, R. H., 1942. The Oceans. Prentice-Hall, Inc., Englewood Cliffs, New Jersey, pp. 584-602.

Thomas, R. W., 1968. Oceanographic Survey Results Off Point Arguello, California, January and November-December 1964. TR 201. U.S. Naval Oceanographic Office, Washington, D.C.

U.S. Naval Oceanographic Office, 1962. Tables of Sound Speed in Sea Water. Special Publication 58. Washington, D.C.

Volkmann, G., Knauss, J., and Vine, A., 1956. The Use of Parachute Drogues in the Measurement of Subsurface Ocean Currents. Transactions, American Geophysical Union. Vol. 37, No. 5, pp. 573.

U.S. Naval Oceanographic Office
OCEANOGRAPHY IN THE CHANNEL ISLANDS AREA OFF SOUTHERN CALIFORNIA, SEPTEMBER AND OCTOBER 1965. June 1968. 50 p., including 33 figs., 1 table. (TR-203)

This report is a detailed environmental study of a survey conducted in the Channel Islands area off southern California in September and October 1965.

Major emphasis is on currents, sound velocity structure, and bottom composition.

1. Oceanography
2. Channel Islands Area
3. Currents
4. Ship - USNS DAVIS (T-AGOR 5)

i. Title: Oceanography in the Channel Islands Area Off Southern California, September and October 1965

ii. Authors: Samuel G. Tooma, Jr. and Harry Iredale, III

iii. TR 203

U.S. Naval Oceanographic Office
OCEANOGRAPHY IN THE CHANNEL ISLANDS AREA OFF SOUTHERN CALIFORNIA, SEPTEMBER AND OCTOBER 1965. June 1968. 50 p., including 33 figs., 1 table. (TR-203)

This report is a detailed environmental study of a survey conducted in the Channel Islands area off southern California in September and October 1965.

Major emphasis is on currents, sound velocity structure, and bottom composition.

1. Oceanography
2. Channel Islands Area
3. Currents
4. Ship - USNS DAVIS (T-AGOR 5)

i. Title: Oceanography in the Channel Islands Area Off Southern California, September and October 1965

ii. Authors: Samuel G. Tooma, Jr. and Harry Iredale, III

iii. TR 203

U.S. Naval Oceanographic Office
OCEANOGRAPHY IN THE CHANNEL ISLANDS AREA OFF SOUTHERN CALIFORNIA, SEPTEMBER AND OCTOBER 1965. June 1968. 50 p., including 33 figs., 1 table. (TR-203)

This report is a detailed environmental study of a survey conducted in the Channel Islands area off southern California in September and October 1965.

Major emphasis is on currents, sound velocity structure, and bottom composition.

1. Oceanography
2. Channel Islands Area
3. Currents
4. Ship - USNS DAVIS (T-AGOR 5)

i. Title: Oceanography in the Channel Islands Area Off Southern California, September and October 1965

ii. Authors: Samuel G. Tooma, Jr. and Harry Iredale, III

iii. TR 203

U.S. Naval Oceanographic Office
OCEANOGRAPHY IN THE CHANNEL ISLANDS AREA OFF SOUTHERN CALIFORNIA, SEPTEMBER AND OCTOBER 1965. June 1968. 50 p., including 33 figs., 1 table. (TR-203)

This report is a detailed environmental study of a survey conducted in the Channel Islands area off southern California in September and October 1965.

Major emphasis is on currents, sound velocity structure, and bottom composition.

1. Oceanography
2. Channel Islands Area
3. Currents
4. Ship - USNS DAVIS (T-AGOR 5)

i. Title: Oceanography in the Channel Islands Area Off Southern California, September and October 1965

ii. Authors: Samuel G. Tooma, Jr. and Harry Iredale, III

iii. TR 203

UNCLASSIFIED

Security Classification

DOCUMENT CONTROL DATA - R & D

(Security classification of title, body of abstract and indexing annotation must be entered when the overall report is classified)

1. ORIGINATING ACTIVITY *(Corporate author)*

U. S. NAVAL OCEANOGRAPHIC OFFICE

2a. REPORT SECURITY CLASSIFICATION

UNCLASSIFIED

2b. GROUP

3. REPORT TITLE

OCEANOGRAPHY IN THE CHANNEL ISLANDS AREA OFF SOUTHERN CALIFORNIA - SEPTEMBER AND OCTOBER 1965

4. DESCRIPTIVE NOTES *(Type of report and inclusive dates)*

Technical Report 16 September to 15 October 1965

5. AUTHOR(S) *(First name, middle initial, last name)*

SAMUEL G. TOOMA, JR.
HARRY IREDALE, III

6. REPORT DATE	7a. TOTAL NO. OF PAGES	7b. NO. OF REFS
June 1968	50	22

8a. CONTRACT OR GRANT NO.	9a. ORIGINATOR'S REPORT NUMBER(S)
b. PROJECT NO. 202	TR 203
c.	9b. OTHER REPORT NO(S) *(Any other numbers that may be assigned this report)*
d.	

10. DISTRIBUTION STATEMENT

Distribution of this document is unlimited.

11. SUPPLEMENTARY NOTES	12. SPONSORING MILITARY ACTIVITY
	U. S. Naval Oceanographic Office

13. ABSTRACT

The Naval Oceanographic Office conducted an oceanographic survey in the Channel Islands area aboard USNS DAVIS (T-AGOR 5) during September and October 1965. The survey was a detailed environmental study with major emphasis on currents, sound velocity structure, and bottom composition. Physical, chemical, geological, and biological data were collected.

Seaward decreases in surface temperature and salinity depicted the influence of the cold, low salinity California Current on the survey area. The sound channel was bottom bounded due to the shallow depths, and the sound velocity axis occurred at a depth of 850 meters (2800 feet). Surface duct development was weak and usually restricted to the upper 10 meters (30 feet).

Data from repeated Nansen casts at anchor stations revealed temperature, salinity, and sound velocity to oscillate in a sinusoidal manner throughout a day. This oscillation is attributed to a combination of internal waves, tidal forces, and the earth's rotational forces.

Current data from parachute current drogues, current meters, and computed dynamics showed the San Nicolas Basin to be the center of a counterclockwise gyre. Maximum current speeds of about 25 cm/sec occurred around the basin periphery. Lesser speeds existed towards the center of the basin and with increasing depth. Current meters, planted 2 miles northeast of San Nicolas Island, indicated a clockwise rotational water movement produced by the tides.

Both bottom sediment analyses and bottom photographs showed the survey area to have the same general characteristics as have been observed in previous studies. Fine-grained, green-gray muds of high organic content were found in depressions, and somewhat coarser materials were found on elevations.

From one plankton collection in September and several in October, a study of the abundance of various plankters suggested that the autumnal decline occurred between 23 September and the second week of October.

DD FORM 1 NOV 65 1473 (PAGE 1)

S/N 0101-807-6801

UNCLASSIFIED

Security Classification

14. KEY WORDS	LINK A		LINK B		LINK C	
	ROLE	WT	ROLE	WT	ROLE	WT
OCEANOGRAPHY						
CHANNEL ISLANDS AREA						
CURRENTS						
SOUND VELOCITY STRUCTURE						
BOTTOM COMPOSITION						